Environmental Earth Sciences (2024) 83:427
https://doi.org/10.1007/s12665-024-11733-9

REVIEW ARTICLE

Implications and problems of research on salt precipitation during CO_2 injection into saline sandstone: a comprehensive review

Luo Chao[1,2] · Yuan Jialin[2] · Zheng Zihao[2] · Feng Chaofu[2] · Li Songze[2] · Yin Nanxin[2] · Chen Cen[2] · Lin Hun[2]

Received: 19 February 2024 / Accepted: 23 June 2024 / Published online: 3 July 2024

Abstract

Carbon capture, utilization and sequestration (CCUS) technology is considered an effective technology for reducing anthropogenic carbon dioxide emissions into the atmosphere. Saline aquifers are the most promising places for CO_2 storage. However, field practice has demonstrated that salt precipitation near wellbores could lower reservoir permeability and result in a loss of CO_2 injectivity. This paper reviews the research progress on salt precipitation during CO_2 injection into saline aquifers. First, the mechanism of salt precipitation is studied in terms of the CO_2 injection stage division and salt precipitation occurrence characteristics. Second, the current technical approaches for salt precipitation research are examined, encompassing numerical simulations, core tests and analytical solutions, and the accomplishments and advancements of these three methods are analyzed. The factors that govern salt precipitation, such as reservoir heterogeneity, salinity, injection rate, temperature, and wettability, are also analyzed. Eventually, the current state of CO_2 storage in saline sandstone is presented, and a number of problems in salt precipitation research are identified.

Keywords Research progress · Salt precipitation · CO_2 injection · Highly heterogeneous · Saline sandstone

Introduction

Saline aquifers are considered the most suitable places for CO_2 storage due to their wide distribution, large volume, and proximity to CO_2 emission sources (Ott et al. 2011). According to the evaluation, the total CO_2 storage potentials of global and Chinese deep saline aquifers are at least 10×10^{15} and 1.435×10^{14} kg, respectively (Cui et al. 2023). Since the Sleipner project's first commercial application of CO_2 sequestration in deep saline aquifers, many CO_2 sequestration projects have been carried out worldwide. To achieve peak CO_2 emissions by 2030 and carbon neutrality by 2060, China's oil and coal companies are vigorously carrying out deep-salt CO_2 sequestration projects (Jiang et al. 2023). For example, the Shenhua Group, the largest coal production company, plans to carry out a 3×10^6 t CO_2 geological sequestration project in a saline aquifer in the Ordos Basin, China, in the next two years (Xu et al. 2022).

High injectivity is critical to carbon capture, utilization and sequestration (CCUS) projects because large amounts of CO_2 must be stored for long periods. The well injectivity is affected by the reservoir porosity, permeability, thickness, and area (Liu et al. 2013). The injection of CO_2 into saline aquifers leads to two processes that may affect the injectivity. First, CO_2 dissolves in saline to form carbonic acid, which may lead to mineral dissolution and precipitation (Smith et al. 2013). In this case, the variation trends of the rock permeability and porosity are closely related to the rock mineralogy, injection rate, rock pore geometry, thermodynamic conditions, and fluid composition (Izgec et al. 2008). Another particular concern is the evaporation and salting-out of water caused by gas injection, which is a physical process that occurs near the injection well. A large amount of dry CO_2 continues to be injected near the injection well, and the salt solution in the saline aquifers continues to evaporate and reach supersaturation, resulting in salt precipitation. The salting-out process causes pore plugging, reduces the porosity and permeability of the reservoir, and

✉ Luo Chao
lc_121989@163.com

[1] State Key Laboratory of Shale Oil and Gas Enrichment Mechanisms and Effective Development, Beijing 100083, China

[2] Chongqing University of Science & Technology, Chongqing 401331, China

seriously affects the CO_2 injectivity, as shown in Table 1 (Xu et al. 2022; Cui et al. 2023).

Strong evidences on the occurrence of salt precipitation primarily have come from field observations of gas injections or storage. Kleinitz et al. (2001) reported gas wells used for gas storage in northern Germany, where NaCl precipitates were detected during well testing by pressure draw-down. A case-in-point is the Ketzin Field, Germany, where it was discovered, through a combination of radiometric pulsed neutron-gamma (PNG) logging and extended saturation modeling, that water evaporation (ultimately resulting in halite precipitation) caused an unusually high CO_2 saturation in a near-wellbore formation (Baumann et al. 2014). Another suspected case of salt precipitation was in the Snøhvit Field. Here, significant pressure buildup was encountered during CO_2 injection into a near-wellbore formation (Grude et al. 2014). This was caused by an unusually low permeability zone around this region, which in turn was suspected to be a consequence of salt precipitation, leading to injectivity loss. A mixture of methyl ethyl glycol and

Table 1 Salt precipitation in typical CO_2 flooding experiments (edited from Cui et al. 2023)

Researher	Porosity and permeability	Water composition	Temperature and pressure	Analysis technics	Variation in porosity and permeability after salt precipitation
Muller et al. (2009)	K = 100mD φ = 0.2	25 wt%NaCl	35°C/6.3 MPa	SEM、ESEM	60% reduction in permeability
Wang et al. (2009)	K = 79mD φ = 0.18	25 wt%NaCl	50°C/8.2 MPa	SEM、ESEM	50% reduction in CO_2 permeability
Bacci et al. (2011)	K = 7.78mD φ = 0.23	26.4 wt%NaCl	45°C/8 MPa	ICP-AES	3% reduction in porosity, 75% reduction in permeability
Oh et al. (2013)	K = 170mD φ = 0.2	15 wt%NaCl	45°C/10 MPa	X-ray、SEM	Local salt precipitation near injector
Ott et al. (2013)	K = 170mD φ = 0.2	34 wt%NaCl	110°C/11 MPa	μCT	Reduction in CO_2 permeability
Peysson et al. (2014)	K = 74mD φ = 0.218	3.5 wt%NaCl(55%KCl and 45% KI)	80°C/change in pressure	X-ray	Local salt precipitation near injector, and 70% reduction in CO_2 permeability
Peysson et al. (2014)	K = 0.01mD φ = 0.214	Brin in Paris Basin	90°C、120°C/ change in pressure	X-ray	Local salt precipitation near injector, and 50% reduction in permeability
Tang et al. (2015)	K = 200mD φ = 0.3	20 wt%NaCl	100°C/1 MPa	SEM	14.6% reduction in porosity, 83.3% reduction in permeability
Ott et al. (2015)	K = 200mD φ = 0.3	20 wt%NaCl	50°C/10 MPa	X-ray、SEM	Uniform salt precipitation and CO_2 permeability increase
Sokama et al. (2018)	K = 90-105mD φ = 0.17–0.19	7.5–15 wt%NaCl	50°C/10 MPa	—	10-35% reduction in permeability
Edem et al. (2020)	K = 200-315mD φ = 0.19–0.2	5–25 wt%NaCl	45°C/6.9 MPa	SEM	0.75-16% reduction in porosity, 10–70% reduction in permeability
Ott et al. (2021)	K = 30-300mD φ = 0.13–0.19	6–28 wt%NaCl	110°C/11 MPa	SEM	Permeability decreases by 1–3 orders of magnitude
He et al. (2024)	K = 0.3-8.7mD φ = 0.099–0.58	286,999 mg/L total dissolved solid	/	SEM、EDS	Porosity decreased by an average of 25%, permeability decreased by an average of 43%

water had to be injected to stimulate the well (Grude et al. 2014). In most of these cases, a dramatic injectivity loss has been reported.

Besides that, numerical simulation and analysis results indicate that the injection capacity may be significantly reduced due to salt precipitation near injection wells (Tambach et al. 2015). Through numerical studies, Giorgis et al. (2007) demonstrated that the injection rate plays a key role in controlling the salt precipitation process and reducing the injection capacity. Muller et al. (2009) demonstrated through numerical studies that a short freshwater prefush (several hours) prior to CO_2 injection can mitigate the adverse effects of salt precipitation on the injection capacity. Numerical calculations conducted by Kim et al. (2012) show that the degree of salting out is proportional to the salinity of the brine. Experimental studies are essential to better identify the key parameters and mechanisms of well injection capacity and to obtain meaningful results from numerical and analytical solutions. Zuluaga et al. (2003) simulated water evaporation by injecting methane into consolidated sandstone cores. Peysson et al. (2014) injected nitrogen into consolidated sandstone cores to characterize water evaporation and salt precipitation. These experimental studies confirm that the injection of dry gas can reduce the injection rate of the saline layer. However, these results cannot be directly generalized to CO_2 injection scenarios because the thermodynamic and flow properties of CO_2, such as the density, viscosity, heat capacity, interfacial tension, and reactivity, are quite different from those of methane and nitrogen, and they have a significant impact on the evaporation process (Bacci et al. 2011a).

In recent years, many scholars have conducted experimental studies on the injection loss caused by salt-out precipitation after supercritical CO_2 injection into sandstone cores (Bacci et al. 2011b; Oh et al. 2013; Ott et al. 2011). Bacci et al. (2011b) conducted four consecutive saline injection and CO_2 flooding tests on the same sandstone core and observed varying degrees of porosity and permeability changes. Their results showed that a small reduction in the porosity can lead to a significant reduction in the permeability of up to 86%. Oh et al. (2013) observed that fractured cores have twice the injection capacity of homogeneous cores, and salt deposits near the injection end of the core were detected via changes in the X-ray intensity. Ott et al. (2011) found through experiments that although the absolute permeability decreased, the relative permeability increased during the tests. Golghanddashti et al. (2013) concluded that the absolute permeability plays a key role in controlling the change in the relative permeability caused by salt precipitation.

There are still many challenges in injecting CO_2 into multilayer, highly heterogeneous saline aquifers, such as those in the Ordos Basin, China (Ren et al. 2021). The multilayer strongly heterogeneous saline aquifers exhibit rapid sedimentary facies changes and poor connectivity (Fig. 1). These characteristics may cause more severe salting-out effects. Therefore, accurately understanding the mechanism of salt precipitation and the influence of various factors on the salting-out near the wellbore is an important scientific problem to improve the injection efficiency of saline aquifers. However, owing to the absence of a sound salting-out mechanism, diverse works have provided conflicting results regarding the various factors that affect the characteristics

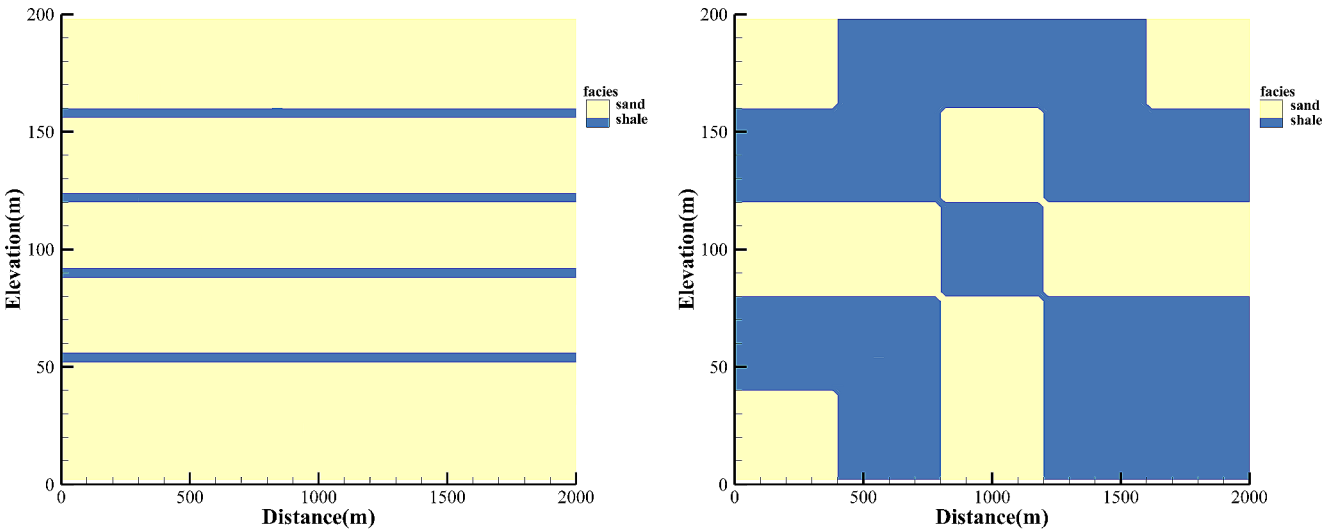

Fig. 1 Enhanced presentation of Single-scale heterogeneity models includes: (**a**) Single-scale interlayer heterogeneity model: This model explores variations within individual layers of a geological formation. (**b**) Single-scale multi-facies heterogeneity model: This model accounts for distinct facies within a reservoir, each adding unique characteristics to overall reservoir heterogeneity. (Edited from Ren et al. 2021)

of salt precipitation. And since there are few review articles, we find it useful to provide an overview of the latest technologies. The aim is to summarize the results of previous studies and clarify how salt precipitation affects the CO_2 injectivity. In addition, we will clarify the potential implications and problems of research on CO_2 storage salt precipitation in saline sandstone.

Salting-out mechanism

Division of CO_2 injection stages

Notably, the supercritical two-phase CO_2–brine seepage process is very complex and involves physical processes such as two-phase flow and two-phase interface movement in porous media (Qanbari et al. 2012; Celia et al. 2011). In contrast to natural evaporation and drying, there are two coupling mechanisms for the change in water saturation in saline aquifers: viscous displacement and drying (Peysson et al. 2014). The time-scale separation between dominant viscous displacement and dominant evaporation is good (Ott et al. 2021). Viscous displacement (which does not lead to precipitation) and water evaporation (which leads to solute enrichment and eventually to salt precipitation) primarily occur on different time scales: viscous displacement occurs over several minutes, while evaporation and precipitation occur over several hours (Ott et al. 2021). According to the different time effects of viscous displacement and drying, three stages of salting out after CO_2 injection occur: advection-leading, transition-leading, and diffusion-leading evaporative drying stages (Wang et al., 2014; Zhang et al., 2016). The transition that occurs from advection- to diffusion-confined flow is direct evidence of reverse solute diffusion. The solute diffuses upward from the low-concentration region of the water phase to the highly concentrated evaporation front. Due to solute accumulation at the brine/supercritical CO_2 interface, salt deposition eventually occurs (Dayo et al. 2021). The drying rate, i.e., the mass of water removed from the sample surface per unit time, can be used to better analyze evaporation in porous media (Baumann et al. 2014). According to the brine production characteristics and the shape and slope of the drying rate curve, the action characteristics of the coupling mechanism in the CO_2 injection stage can be identified. In the initial stage of supercritical CO_2 injection, CO_2 breakthrough quickly occurs. The sharp decrease in the slope of the pressure difference after breakthrough is due to the high contrast between the viscosities of supercritical CO_2 and brine. Bacci et al. (2011b) also reported that large residual water saturation is caused by the large difference between the viscosities of supercritical CO_2 and brine. This may result in early gas invasion and poor brine displacement efficiency. A higher drying rate leads to the rapid precipitation of salt, and the production of brine and steam increases dramatically. With the passage of CO_2 displacement brine, the contribution of advection gradually decreases, and diffusion flow dominates (Dayo et al. 2022). The generation rate of brine and steam decreases, the generation of brine eventually stops at a certain stage, and evaporation becomes the main mechanism of action. The decrease in steam generation is mainly affected by three factors. First, as CO_2 injection progresses, the salinity of the brine in the porous medium increases. In contrast to the constant evaporation rate of deionized water, when the salinity of the brine increases, the permeability potential increases, and the activity coefficient decreases (Hassan et al. 2018). According to Raoult's law, a decrease in water activity leads to a decrease in water evaporation. Second, most of the brine that can evaporate is produced early on. The amount of brine remaining affects the rate of evaporation. In the initial stage of CO_2 injection, the brine production in the largest pores of the rock sample is caused by CO_2 flow. When the driving force of CO_2 cannot overcome the capillary force of the small pore throat, the nonwet phase CO_2 flow has no flow trend, so it is difficult to produce new brine. In addition, more brine production reduces the chance that the remaining brine will come into contact with the CO_2 flow (Fig. 2), which in turn reduces the evaporation rate in the later stages of CO_2 injection (Javed et al., 2016). Third, in a later stage, when the solubility limit is reached, the salt precipitates. Precipitation reduces the connectivity of the surface water film, leading to a decrease in the evaporation rate (Fujimaki et al. 2006).

In addition, some scholars have divided the injection stages according to the variation in the amplitude of the reservoir permeability during CO_2 injection. For example, Zhang et al. (2019a) studied the influence of formation water flow on salt precipitation by conducting tight sandstone water flooding experiments. They noted that salt precipitation during the pressure reduction process can be divided into three stages. In the first stage, that is, the initial precipitation stage, the salt in the formation begins to precipitate obviously, the salt precipitation dramatically reduces the permeability of the core, and the maximum permeability reduction range is 35–67%. The second stage is the precipitation equilibrium stage (10–3 MPa), and the decrease in the permeability is not large (less than 5%). In the third stage, the salting-out intensification stage, the permeability decreases further. The degree of damage to the permeability of the core by salt precipitation increases to more than 90%.

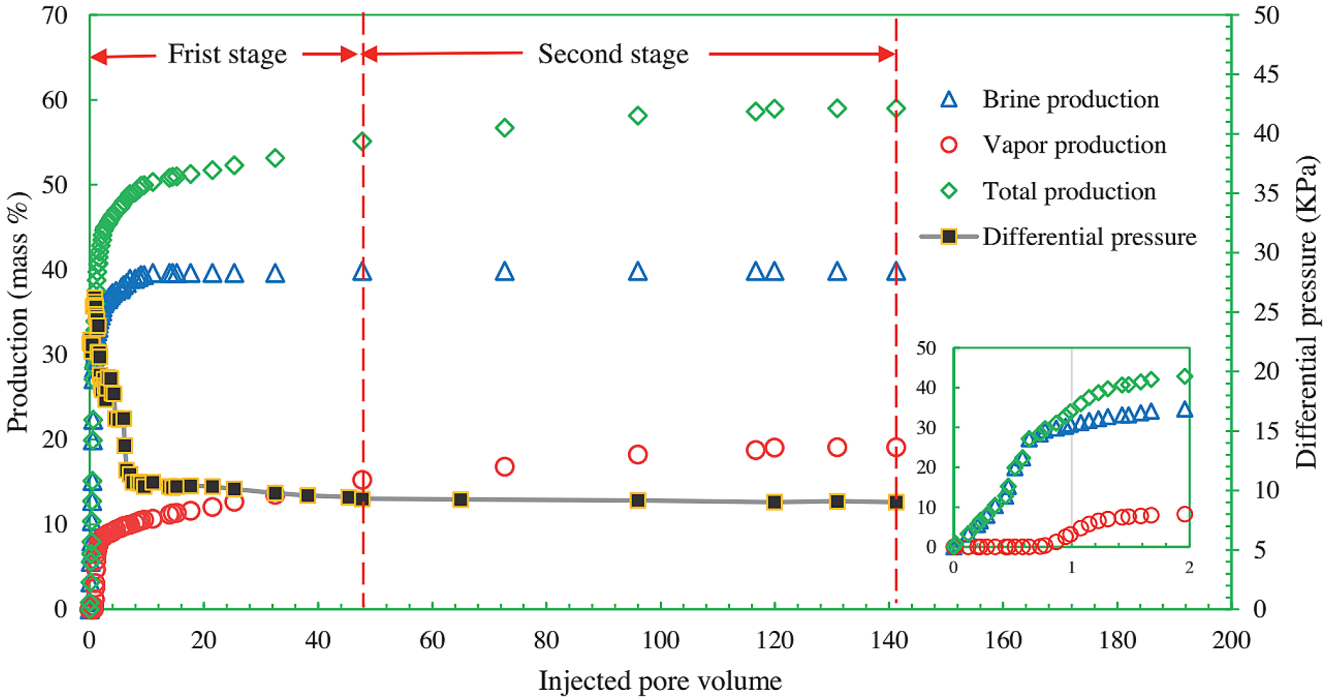

Fig. 2 Fluid production and pressure curves during second flooding test. (Edited from Javed et al., 2016)

The characteristics of salt precipitation

Two main types of precipitation form near the well: nonlocal salting-out near the well and local salting-out under the drying front (Meng et al. 2015). The formation processes of the two types of precipitation are different, and they have different periods. Core experiments have also confirmed that the salting-out profile of the rock sample was uneven, and the salting-out was more concentrated near the sample inlet surface (Javed et al., 2016).

The time scale of the drying determines the crystallization process, and the drying time is caused by the rate of water transport in the injected fluid phase, which is determined by the solubility limit of water in the injected fluid phase and the injection rate. The amount of sediment depends on the nonflowing portion of the brine that eventually dissolves in the CO_2-rich phase (Ott et al. 2021). The localized salting-out below the drying front mainly occurs at the corners of the $scCO_2$-filled pores that were previously filled with saline. Pores with an equivalent pore size of <50 μm are classified as small pores, those with an equivalent pore size of >200 μm are classified as large pores, and those with an equivalent pore size of 50–200 μm are classified as medium pores. There are different views as to where salting-out occurs, i.e., in small or large pores. One view is that the pores that are completely filled with salt are few and mainly occur in pore throats (Fig. 3) that cannot be invaded by $scCO_2$ to a lesser extent (Dayo et al. 2021). In medium wet sandstone, salt is mainly deposited in small pores and in the nooks and crannies of large and medium pores filled with supercritical CO_2. Salt precipitation is more even in sandstones than in carbonate rocks (Dayo et al. 2022). Another view is that the salt mainly comes from the microporous system and only precipitates in the macroporous system, but it does not precipitate in the microporous system. This is because CO_2 that is already saturated with water enters the micropore domain as a result of the equilibrium solubility model, which prevents evaporation in the micropore (Ott et al. 2021).

In addition, capillary action and the rate of water evaporation determine the flow state, which determines the direction of solute transport (cocurrent or countercurrent), thus affecting the macroscopic distribution of local precipitation in the lower part of the drying front (Ott et al. 2021). The Peclet number, that is, the ratio of the advection rate to the diffusion rate, can better define the distribution of salt precipitation in rock samples (Peysson 2012; Roels et al. 2014). When $Pe \ll 1$, diffusion is the main process, and the salts are uniformly precipitated in the porous medium. When $Pe = 1$, advection is greater than diffusion, and salt precipitation is uneven (Huinink et al. 2002). Kim et al. (2013) conducted pore scale experiments on salting-out and determined that salting-out can be divided into two types: an isolated single-crystal structure and an aggregated polycrystalline structure.

For semiclosed systems, in addition to these two types of precipitation, a third type of solid precipitation occurs at the interface between the reservoir and the seal (Meng et al. 2015).

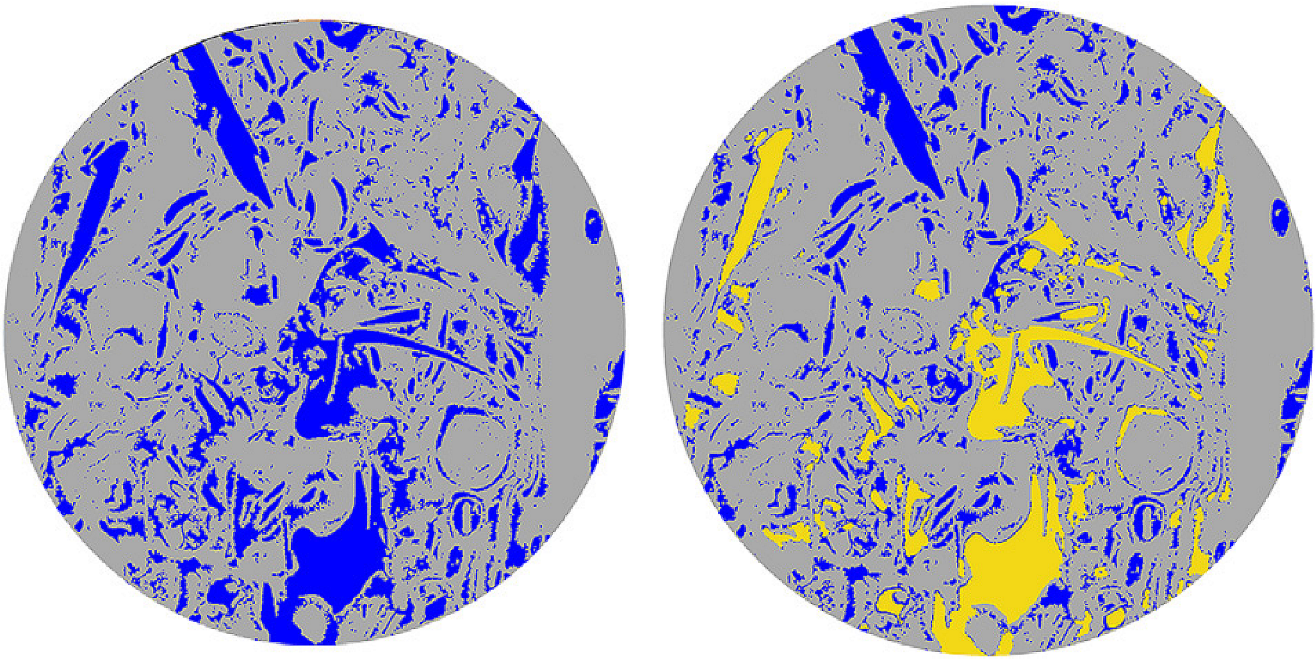

Fig. 3 Microscopic photos of the reservoir for vacuum saturation (left) and $scCO_2$ displacement (right). (Edited from Dayo et al. 2021)

Causes of salt precipitation

There is controversy regarding whether the salting-out position is the water phase or the gas phase. Although salt crystals grow at different rates, they generally grow in both the liquid and gas phases (Miri et al. 2015). Liu et al. (2013) noted that the key assumption about the pore-permeability relationship after salting out is that salt precipitation in water occupies the pore space. They concluded that the salt was initially dissolved in the water and could only be precipitated from it. Ott et al. (2015) used micron-CT imaging to study the distribution of solid salt after CO_2 displacement and the initial CO_2 in the pore space and found that the overlapping area of the two was less than 5% of the common cross section. The salt precipitates in the residual brine phase near the initial CO_2 occupancy volume, and there is no transport mechanism for liquid water and steam to pass through the CO_2–brine interface or a transport mechanism by which the salt can enter the CO_2 channel (Fig. 4).

Miri et al. (2015, 2016) explored the kinetics of salt precipitation at the pore scale through chip experiments, but they came to the opposite conclusion. They found that salt aggregates attract water from adjacent network particles through a surface energy effect via a continuous film of water surrounding the mineral particles, which allows the evaporation front to continuously absorb fresh brine, thus allowing salt to continue to grow on these aggregates. The result of this mechanism is a large accumulation of salts in the gas phase in the form of aggregates (Fig. 5). Therefore, the salting-out processes and mechanisms can be summarized as follows.

(1) Non-miscible displacement of the original solution by injected CO_2. When CO_2 enters the pore-throat structure of the reservoir, it will result in a two-phase flow, namely the supercritical CO_2 phase and the saline phase. After non-miscible displacement of the original solution forms by injected CO_2, the residual water will exist in the reservoir in the forms of water films and water bridges. In terms of physical boundaries, immiscible two-phase displacement systems can be theoretically divided into three categories (Fig. 6): (i) closed systems in which all of the boundaries are impervious; (ii) open systems with open horizontal boundaries that allow natural brine to flow out; and (iii) semiclosed systems in which the lateral boundaries are impervious to water and the vertical boundaries of the reservoir are surrounded by sealing units with low permeability. The numerical results reveal the different characteristics of the pressure changes in saline aquifers under different boundary conditions. Since different types of precipitation occur near injection wells and have obvious effects on fluid flow, numerical simulation results can be used to compare the interaction between pressure accumulation and fluid saturation in saline aquifers under different boundary conditions (Meng et al. 2015).
(2) Evaporation of water from the solution into the flowing CO_2 phase. Under the continuous flow of dry supercritical CO_2, the water in the solution evaporates into the

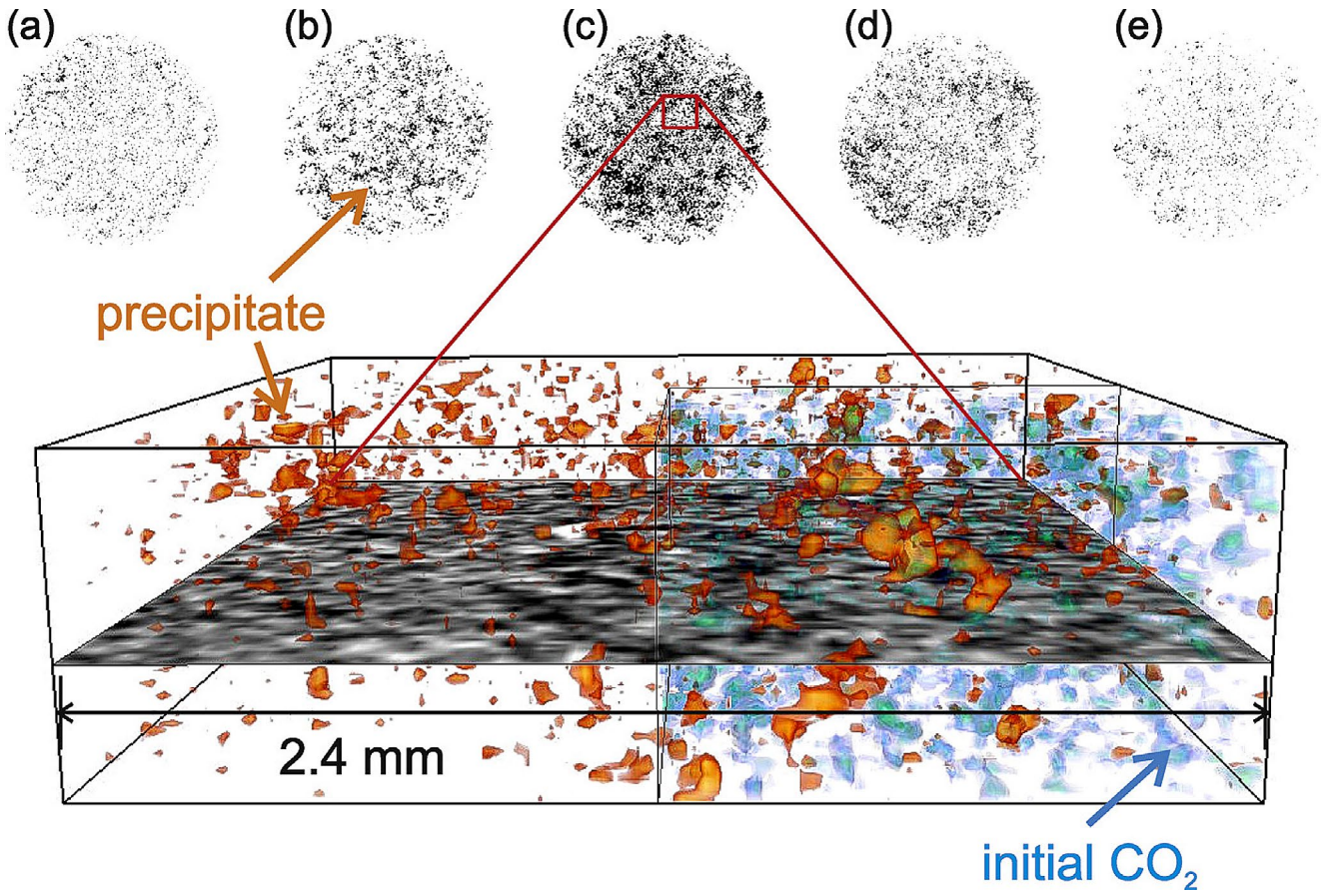

Fig. 4 Microscale μCT data of salt precipitation after CO_2 flooding. (Edited from Ott et al. 2015)

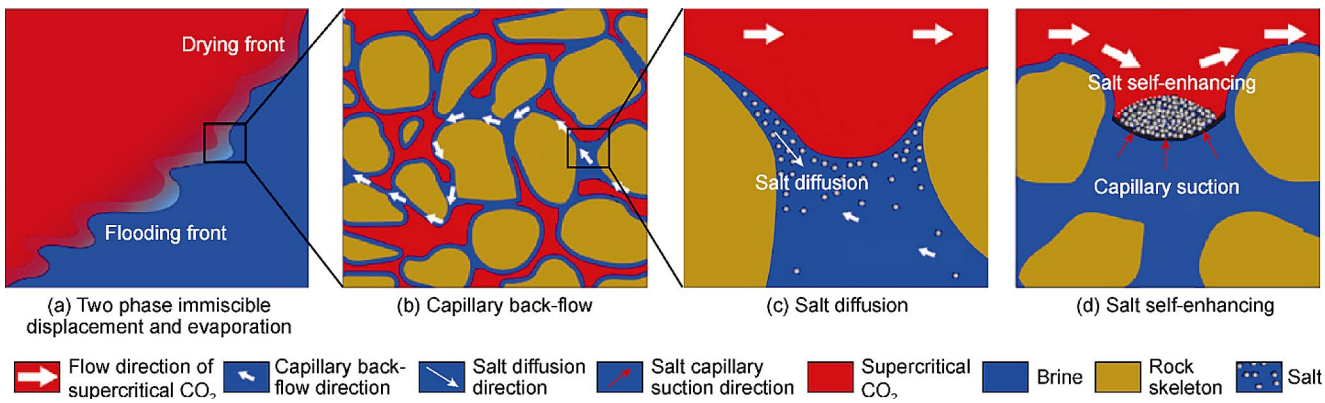

Fig. 5 Mechanism of CO_2 displacement-evaporation-precipitation(Edited from Miri and Hellevang., 2016; Zhang et al., 2024)

flowing CO_2 phase. Under isothermal conditions, the evaporation rate depends on driving forces such as capillary forces and viscous forces (Lehmann et al. 2008; Shokri and Or, 2011). The evaporation of water will enhance the relative permeability of CO_2 and further boost the evaporation process. In current CO_2 injection simulations of saline aquifers, water evaporation is generally considered to be in local thermodynamic equilibrium due to the rapid diffusion of water vapor in pore throats (Peysson et al. 2014). Spycher et al. (2003) established a relatively accurate CO_2-formed water miscibility equation by combining the chemical potential and Redlich–Kwong (R–K) equation of state, and they concluded that the solubility of CO_2 in the water phase was 1–2 mol% and that of water vapor in the CO_2 phase was 3–8 mol% at 100–150 °C and 10–20 MPa. Pruess et al. (2005) applied this equation in TOUGH2 to simulate formation water evaporation during CO_2 injection,

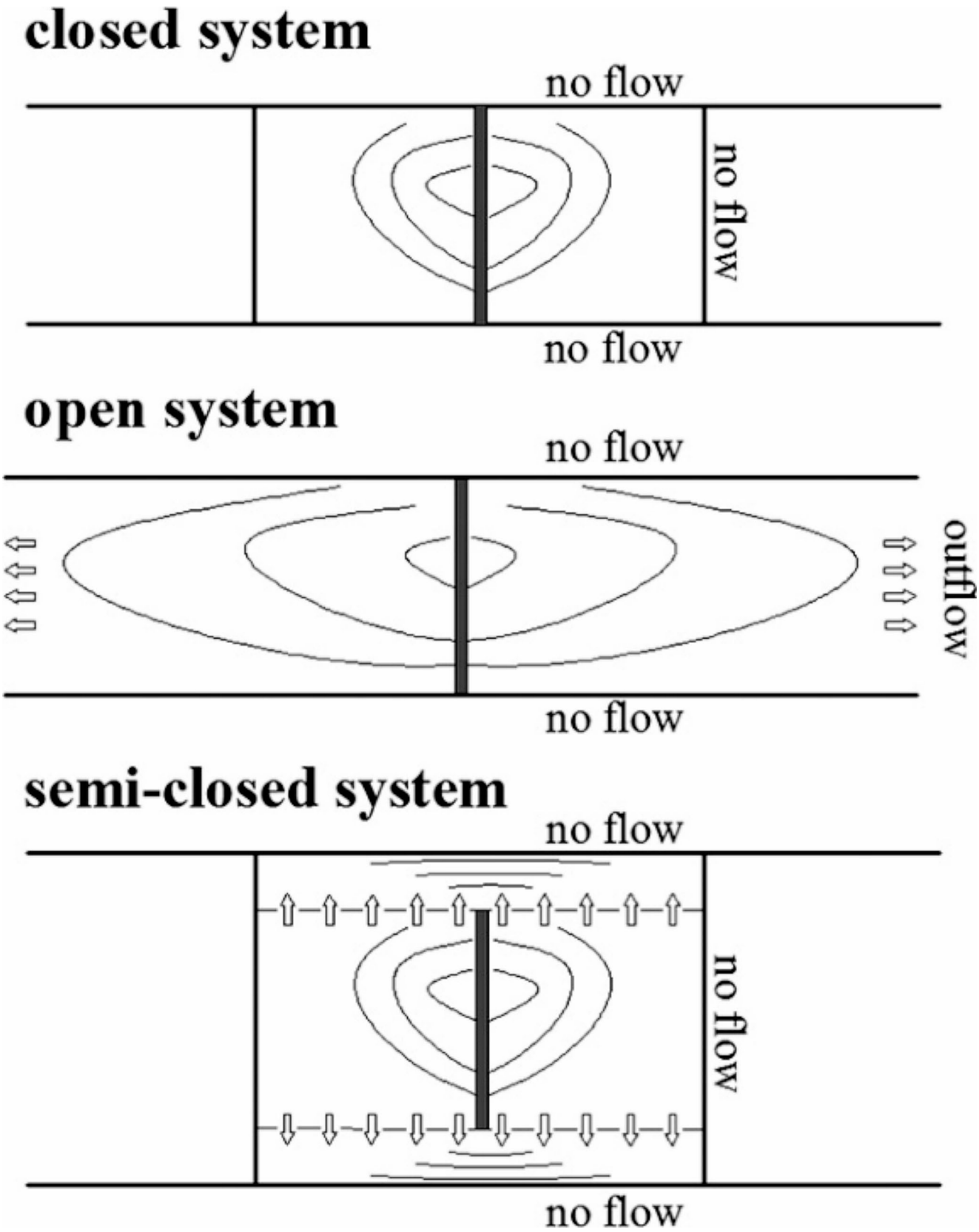

Fig. 6 Enhanced presentation of boundary conditions for the three storage systems: (**a**) Open system; (**b**) Closed system; (**c**) Semi-closed system. (Edited from Meng et al. 2015)

and it has been widely used in CO_2 sequestration studies (Babak et al., 2018) and CO_2-based geothermal exploration (Cui et al. 2018a).

(3) Capillary-driven backflow of the solution towards the injection end. Due to the dry evaporation effect at the displacement front, there is a capillary pressure gradient compared to the high water level in the distant region. The capillary pressure depends on the pore size distribution (PSD). Qing (2021) discussed the difference in the capillary pressures of large and small throats that cause liquid to flow toward the surface of the porous medium, bringing evaporation close to an earlier stage, which is called capillary-driven backflow. When this gradient exceeds the injection pressure gradient, the capillary-driven backflow of solution reverts to the injection end, and the reservoir water returns to the evaporation front, resulting in continuous evaporation. However, achieving capillary pressure is complicated because different minerals have different contact angles and surface tensions, resulting in different residual water saturations (Norouzi et al. 2022).

(4) Solute diffusion in the solution. As the water evaporates into supercritical CO_2, the salt concentration in the residual water increases. This may cause the salt to spread from the dry front to the formation water. Once the salt concentration reaches its solubility limit, the salt will precipitate out of the solution.

(5) Self-enhanced growth of salt. The precipitated salt has a strong affinity for saline and forms an effect similar to capillary force, inducing the distant saline to move towards the evaporation front, and the self-enhanced growth of salt will further increase the precipitation. An important premise of this self-reinforcing mechanism is that there are relatively thick interconnected films on the grain surfaces (Miri et al., 2016; Zhang et al. 2024a). However, the existence of this thick water film and its practical significance in hydraulic conduction need to be studied further.

Salting-out research methods

Numerical simulations

Most existing numerical codes capable of simulating drying and salting-out processes (e.g., Transport of Unsaturated Groundwater and Heat version 2 (TOUGH2; Pruess 1991), DUNES for Multiphase, Component, Scale, Physics, etc. Flow and Transport in Porous Media (DUMUX; Flemisch et al. 2011), Computer Modeling Group (CMG), and Eclipse) are built on the basis of implementing physical processes, which include: (1) immiscible two-phase displacement; (2) the evaporation of brine into a dry CO_2 stream; and (3) capillary-driven water phase reflux.

Laboratory experiments

Core experiments

Core experiments are an important means of understanding the process of CO_2 storage in saline sandstone. Peysson et al. (2014) reported experimental results on rock drying caused by the continuous injection of a large amount of dry gas (N_2), simulated the physical process controlling the decrease in the water saturation of the reservoir rock, studied the slow and fast drying rates and the influence of capillary pressure on drying, and determined the main physical parameters controlling the key mechanism of rock drying. Ott et al. (2015) experimentally studied the effects of the drying process and salt precipitation on the flow rate under actual near-wellbore flow velocity and actual thermodynamic conditions, injected dry $scCO_2$ into salt-saturated siliceous sandstone, and monitored the spatiotemporal evolution of the saturation changes using microcomputed tomography (CT). Javad et al. (2016) injected supercritical CO_2 into sandstone samples fully saturated with NaCl, measured the drying rate, and analyzed the effects of the injection rate and salinity on salt precipitation.

An increasing number of scholars have focused on the differences in salt precipitation between sandstone and other types of rocks, such as carbonate rocks. Peysson et al. (2011) conducted an experimental study on the permeability changes caused by the drying of medium- and high-permeability sandstone and carbonate rocks under different brine conditions and evaluated the effects of the rock type and initial permeability on injection alteration. The type of flow blockage and the spatial redistribution of salt deposits in the pore matrix were investigated. The salt deposits were concentrated near the core surface, and the pores were blocked by solid salt deposits. Dayo et al. (2022) injected supercritical CO_2 into depleted carbonate and sandstone reservoirs and compared the characteristics of salt precipitation development. Their experimental results revealed that the time required for precipitation to begin was shorter in sandstone than in two carbonate samples, indicating that the pore connectivity plays a major role in the evolution of salt precipitation and that the pore connectivity is generally better in sandstones.

With the advancement of technology, the microscopic scale of solute transport, flow geometry, and porous structure can be observed using visual experimental devices (Wang et al. 2023). Lehmann and Or (2009) conducted evaporation experiments on textured media and utilized

neutron transmission and dye pattern imaging to quantify the water distribution and drying front dynamics. Synchrotron X-ray microtomography has been applied to study the pore-scale dynamics of the dissolved salt distribution in three-dimensional dry salt-containing porous media (Shokri 2014). Ott et al. (2014) studied salt precipitation due to CO_2 injection in both single-pore and porous systems under near-well conditions and imaged the saturation and salt deposition using microcomputed tomography. Zhang et al. (2019a, b) studied the influence of salt precipitation/dissolution on the physical properties of tight gas reservoirs through core analysis and core displacement tests; analyzed the influences of the specific area, porosity, pore throat diameter, and other physical properties on the core; and observed the flow state of brine and salt precipitation through microscopic visualization experiments (Fig. 7). Muhammad et al. (2020) studied the effects of the CO_2 injection scheme, rock permeability, brine type, and salinity on the CO_2 injection capacity using X-ray fluorescence (XRF), X-ray diffraction (XRD), and field emission scanning electron microscopy with energy dispersive X-ray spectroscopy (FESEM-EDX). Core samples with different permeabilities from a typical geologically sealed reservoir were analyzed, and the migration of the precipitated salt, silica particles, and kaolinite was observed. In addition, the $CaCl_2$ saline-saturated core was the only sample with increased permeability after the CO_2 displacement experiment. Dayo et al. (2021) studied the pore-scale evaporation and drying process leading to salt precipitation of saturated porous media in brine using high-resolution X-ray microtomography under high-temperature and high-pressure conditions.

The combination of laboratory core experiments and numerical simulations has become a trend in the study of salt precipitation in the process of saltwater storage in sandstone. Mehdi et al. (2009) developed a mathematical model of radial CO_2/brine binary displacement combined with core experiments, established a salt precipitation model for the region where vaporization occurs in a binary system, studied the effect of salt precipitation on permeability, and proposed an analytical solution based on the time-dependent skin factor. Giacomo et al. (2011) designed a supercritical CO_2 core displacement experiment. Salt scaling on the core led to different degrees of changes in the porosity and permeability. A slight reduction in the porosity led to a significant reduction in the permeability, and the porosity decreased from the initial value of 22.59–16.02%. The permeability decreased from 7.78 to 1.07 mD. Based on the petrophysical data, a tube string model of a calibrated vermaspress was established for numerical simulation. Roels et al. (2014) captured gas–solid salt saturation profiles via microcomputed tomography (micro-CT), and the pressure drop above the core was continuously monitored. They compared the observations with numerical simulations conducted using a TOUGH2 reservoir simulator with the EOS module ECO_2N (Roels et al. 2014).

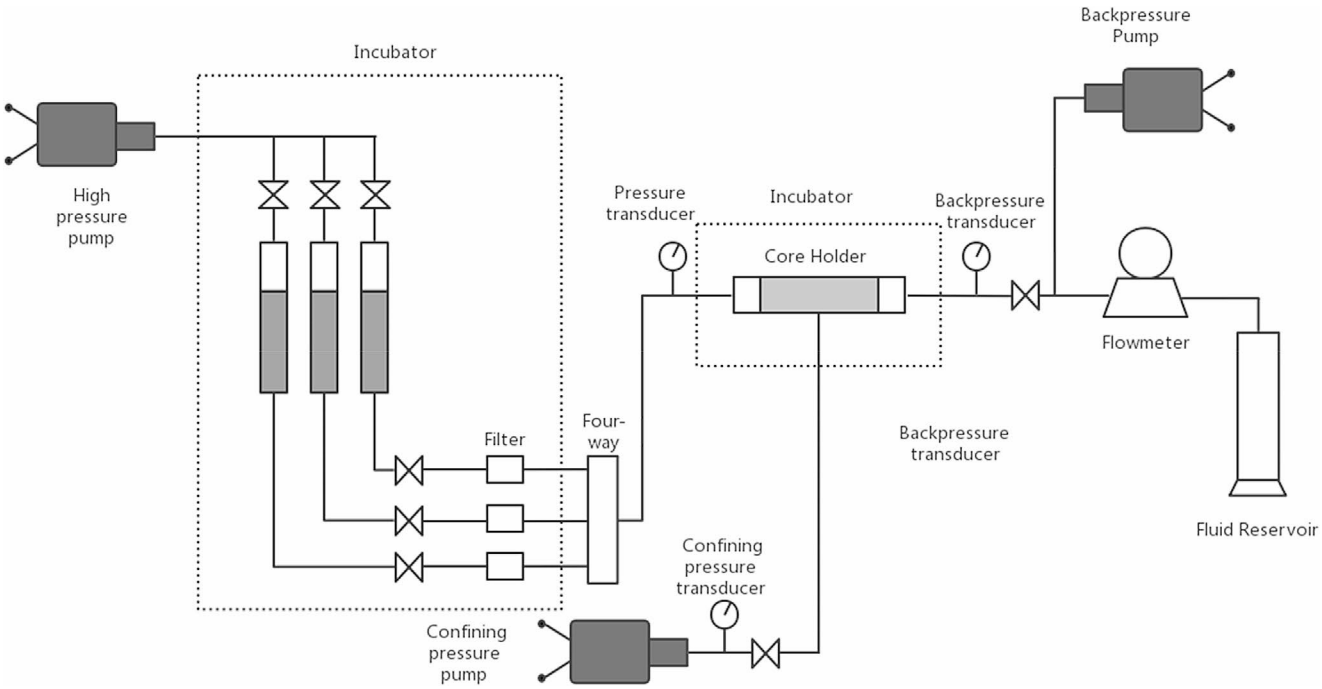

Fig. 7 The experiment setup for core flooding experiments. (Edited from Zhang et al. 2019a, b)

Micro/nanoflow control

Salt precipitation involves complex processes such as CO_2–water seepage, gas–liquid mass transfer, and mineral crystallization (Zhang et al. 2024a). A detailed analysis of the crystallization and precipitation processes of salt in pores is needed to reveal the physical mechanism of salt precipitation. Microscopic visualization experiments are the optimal approach for analyzing the pore-scale dynamics of salt precipitation since they can not only visually observe salt precipitation but also rule out the impact of rock minerals. Kim et al. (2013), Miri et al. (2015), Nooraiepour et al. (2018), and He et al. (2019) studied the kinetic characteristics of salt precipitation at the pore scale with NaCl as the aqueous solution through a series of lab-on-a-chip experiments. They found that salt crystals come in two forms: a single large crystal and a micron-scale aggregate. It is believed that single large salt crystals grow in the liquid phase far from the CO_2 interface and, therefore, do not occupy subsequent CO_2 permeation channels. Due to the fluidity of the water film, micron-scale salt crystals continue to grow, resulting in a large amount of micron-scale salt crystals. The different forms of salt precipitation are related to the uniformity of the pore distribution, and the amount of salt precipitation is related to the mobility of the pore water film (Miri et al. 2015).

In addition, many scholars have used micro/nanoflow control experiments to study the effects of fractures and reservoir heterogeneity on salt precipitation at the pore scale. Jiang et al. (2022) designed a microscopic model to simulate reservoir fractures and conducted pore-scale experiments to study the effects of the CO_2 injection rate, solution concentration, and rock wettability on salt extraction from fractures. Under hydrophilic conditions, reducing the CO_2 injection rate and increasing the solution concentration increase the amount of salt precipitation in the fracture and decrease the injection ability of the micromodel. However, increasing the CO_2 injection rate and rock contact angle greatly reduces the amount of salt precipitation in the fracture and has little adverse effect on the injection ability of the micromodel. He et al. (2023) designed two different structures with vertical heterogeneity and lateral heterogeneity through pore-scale experiments and studied the salting-out phenomena in different heterogeneous structures.

Analytical solutions

Numerical results and laboratory experiments are highly reliant on specific cases and costly in terms of both time and computational expenditures. Nevertheless, analytical solutions can effectively model the CO_2-brine systems and salt precipitation without incurring computational costs. For example, Hesse et al. (2007) developed the Method of Characteristics for investigating the migration of the CO_2 plume after the end of CO_2 injection, or by making use of Darcy's equation as well as a modified Buckley–Leverett theory. McMillan et al. (2008) established a model to determine the CO_2 injectivity within a homogeneous reservoir with constant pressure at the boundaries, based on phase mobilities and the propagation speed of saturation fronts. Zeidouni et al. (2009) established an analytical model and assumed that the precipitated salts were uniformly distributed in the reservoir. Pruess (2009) took into account the absence of capillary pressure and, on the basis of the similarity solution, derived values for the constant solid salt saturation in the dry-out region. A review of these analytical works is presented in Table 2.

However, the current analytical solutions for salting-out are far from adequate. The main assumptions employed in the analytical models are as follows: (1) The reservoir is regarded as homogeneous. (2) Diffusion and dispersion effects are ignored. (3) Capillary and gravitational forces are negligible. (4) Mineral reactions are considered to be negligible. (5) Local phase equilibrium is taken into account and lastly. (6) Temperature and pressure are presumed to be constant (Milad et al. 2017). Norouzi et al. (2022) held the view that there was no analytical solution which took into account "the capillary effects on the propagation speed of saturation shocks and on the salt precipitation" in the dry-out region. There are few available analytical studies attempting to mathematically formulate the saturation distribution within the reservoir while considering mass transfer and minerals/salt precipitation. Based on the provided literature review, the majority of the analytical works in this field only considered simple CO_2-water displacement systems and gravity currents without mass transfer and salt precipitation. Additionally, capillary-driven backflow can considerably increase the amount of precipitated salt near the injection well area (Bacci et al., 2011; Grimm Lima et al., 2020; Norouzi et al. 2021). Salt saturation increases as it gets closer to the injection well, and thus it is not constant (Pruess and Spycher 2007). It is requisite to establish a more realistic model for evaluating the salting-out effect.

Sensitivity of the governing parameters

Reservoir heterogeneity, salinity, injection rate, temperature, as well as wettability all have an impact on the evaporative salting-out of saline sandstone (Cui et al. 2016a).

Table 2 Analytical investigations of CO_2-Brine systems considering Mass transfer and salt precipitation (edited from Norouzi et al. 2022)

Study	Methodology
Nordbotten and Celia (2006)	Developed a similarity solution to find the locations of the interfaces between different saturation regions. Their solution is also able to capture CO_2 density-driven flow.
Noh et al. (2007)	Investigated minerals precipitation inside the reservoir through fractional flow theory and shock waves definition for cases that CO_2 displaced water and water displaced CO_2. Based on graphical solution (drawing tangent lines), they provided equations to calculate the retardation factors and the I and J coordinates of the tangent lines.
Zuluaga and Lake (2008)	Using a constant capillary diffusion coefficient and numerical integration, they proposed a traveling-wave solution to analytically solve water vaporization for dry gas (methane) injection into immobile water.
Pruess (2009)	Used mass balance for the dissolved water into the CO_2 stream and the saturation profiles from the Buckley-Leverett fractional flow theory and proposed an equation that related the average gas saturation inside the dry-out region to the amount of the precipitated salt, which they considered to be constant in the dry-out region.
Zeidouni et al. (2009)	The similar fractional flow approach is used to formulate gas saturation inside a cylindrical reservoir. They also provided equations to estimate salt precipitation inside the dry-out region. However, they suggested a uniform and constant precipitation inside the drying region.
Mathias et al. (2011)	Extended an analytical solution to estimate the pressure buildup within the injection well area, considering water evaporation, CO_2 dissolution into the brine, and salt precipitation. However, they considered negligible capillary pressure in their work.
Kelly and Mathias (2018)	Presented a similarity solution relating capillary pressure and salt precipitation around the injection well. Their results revealed that the amount of the precipitated salt is highly controlled by the capillary strength and that the presence of capillary pressure led to a higher amount of precipitation near injection area.
Norouzi et al. (2022)	Developed an analytical solution based on fractional flow theory and shock waves for CO_2-brine systems considering the effect of capillary pressure. The results emphasize that effects of capillary pressure should not be ignored.

Reservoir heterogeneity

According to the type, reservoir heterogeneity can be divided into interlayer heterogeneity, intralayer heterogeneity, plane heterogeneity, and microscopic heterogeneity (Qiu 1992). The degree of reservoir heterogeneity affects the timing of salting-out, the initial location of salting-out, and the in situ distribution of salting-out (Dayo et al. 2021).

The interaction of multiple layers in a heterogeneous reservoir will affect the distribution of the CO_2 mass flow rate with wellbore depth and thus will affect the corresponding temperature and pressure changes in the wellbore and reservoir. The burial depth, porosity, permeability, and thickness are all important factors affecting the CO_2 mass flow rate in the wellbore. Changes in the CO_2 quality and flow in the wellbore will balance the CO_2 injection pressure by affecting the heat released, compressibility, and potential energy loss of the rock and by changing the hydrostatic pressure and frictional pressure drop of the CO_2, thus changing the temperature of the CO_2 flowing into each layer (Liu et al. 2016). In the process of longitudinal unified multilayer injection, the different permeabilities and porosities of the different saline aquifers lead to the asynchronous movement of the two-phase flow interface, which greatly affects the CO_2 displacement and drying processes and thus affects the final salt precipitation characteristics (Zhou et al. 2008).

For planar heterogeneity, regardless of the CO_2 injection rate, the precipitated salts mainly exist in clusters (Fig. 8). Moreover, the salt distribution is relatively dispersed and has little influence on the injection capacity (He et al. 2023). Cui et al. (2016b) studied the salt precipitation concentration in the area near an injection well under different initial reservoir permeabilities 30 years after CO_2 injection and concluded that the permeability does not have a significant influence on the salting-out volume and that the salting-out volume concentration is basically the same under different permeability conditions (Cui et al. 2016b). Milad et al. (2017) reported that permeability had no effect on the determination of the equilibrium zone in the salt precipitation model, and the permeability only affected the injection capacity. The main parameter that comes into play is the relative permeability, which depends on the nature of the aquifer (Milad et al. 2017). However, other scholars have presented a different view. Reservoirs with medium permeability (50×10^{-3}–250×10^{-3} μm^2) minimize salt accumulation and allow sufficient pressure dissipation and are therefore the best storage media for CO_2 injection (Qing et al., 2021). The higher the permeability of the rocks is, the longer the residence time between the CO_2 and brine/rocks due to the larger pore size, and the greater the damage (Mohammad et al., 2020).

At present, few studies have been conducted on the effect of within-layer heterogeneity on salting-out. Core experiments have focused on the characteristics of salt precipitation in the X and Y directions, and less research has been conducted on the vertical rhythm and vertical structure changes in a single layer during the salt precipitation process. In the actual CO_2 injection process, due to the density difference between the CO_2 and brine, more salting-out may occur at the bottom of the sandstone layer. However, both the numerical and analytical solutions underestimate the amount of permeability reduction. This could be due to several reasons, such as the uniformity of the reservoir parameter settings in the analytical/numerical case and/or

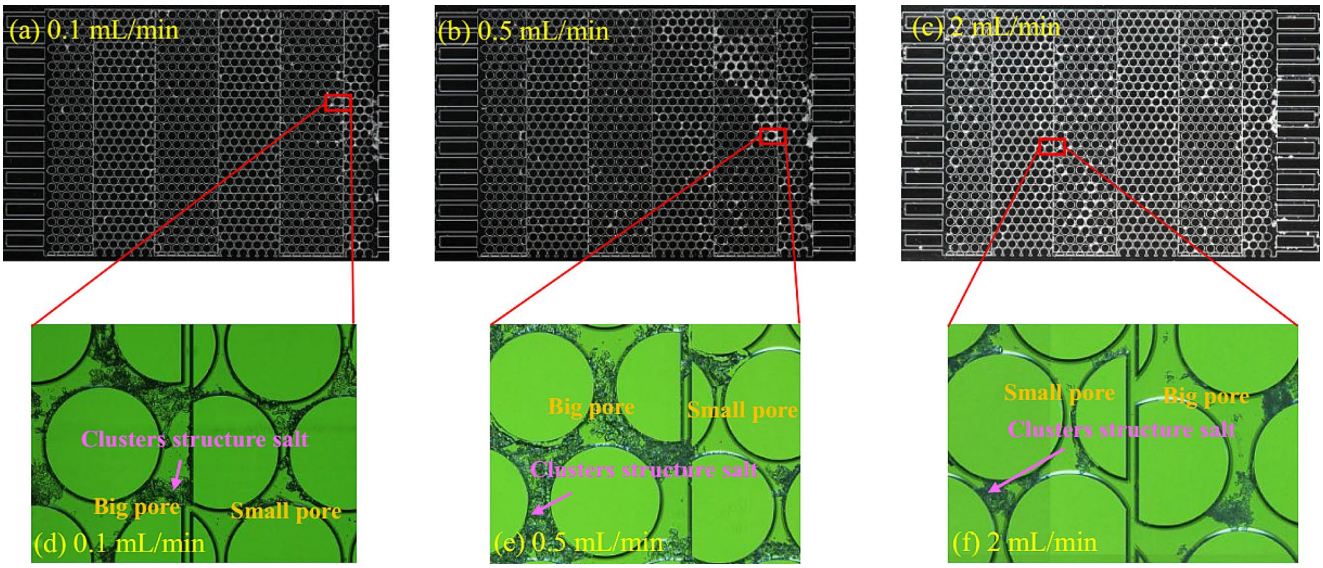

Fig. 8 Salt distributions under different CO_2 injection rates in heterogeneous structure (Edited from He et al. 2023)

the lack of a Z direction in the model. This eliminates the accumulation of salt at the bottom of the reservoir due to factors such as gravity and intralayer heterogeneity, which exacerbates the reduction in permeability.

In terms of microheterogeneity, the main concern is the effects of the PSD, self-enhancement, and microfractures on salt precipitation. In the gas phase, micron-sized crystals aggregate to form a microporous medium with numerous capillaries. These micropores can absorb brine strongly over a long distance to the evaporation front through a film of water connected by capillaries. The brine absorbed in the salt structure is several orders of magnitude thinner than the brine captured in the pores. Due to its high surface area-to-volume ratio, it quickly becomes highly supersaturated, resulting in high nucleation rates and the formation of additional salt crystals. The resulting salt provides additional surface area for evaporation, thus increasing the overall salting-out rate. This mechanism occurs even at extreme CO_2 flow rates. Therefore, salting-out formation may be more severe than has been previously concluded based on core flooding experiments and numerical simulations alone (Miri et al. 2015). It should be noted that when CO_2 leaks in a fracture, the salt tends to grow until the fracture is plugged (Zhang et al., 2023; Chen et al. 2024). This is of great significance to the self-healing of fractures in the cap layer.

Salinity

Aquifer salinity mainly affects the formation of salt and controls the occurrence and extent of precipitation (Parvin et al. 2020). Brine salinity has been shown to be a factor affecting rock wettability, i.e., a higher brine salinity leads to more carbon dioxide wetting the rock. An increase in the salinity of the brine will lead to a slight decrease in the solubility of the water in the CO_2 phase, thereby reducing the evaporation rate. An increase in salinity leads to a decrease in the residual and dissolved captured CO_2 and an increase in the mobility of CO_2 (Emad et al. 2017), resulting in a significant decrease in the dissolution of CO_2 in brine. A salinity sensitivity analysis revealed that the higher the salinity is, the more salt precipitation occurs, and the greater the reduction in the porosity. When the salinity is less than 5%, the salt deposition and permeability damage are negligible (Grude et al. 2014). These results are in good agreement with field observations. For example, for low-salinity and high-permeability reservoirs, such as the Utsira Formation in the Sleipner Field in the North Sea (salinity of 3.5% and permeability of 1 D), there have been no reports of impaired injection capacity or well plugging in the field to date. However, for the Katzian reservoirs, salt precipitation is the main cause of pressure buildup during CO_2 injection into high-salinity (25%) and medium-permeability (~100 mD) reservoirs (Grude et al. 2014).

The CO_2 displacement efficiency is a single function of the difference in the viscosities of CO_2 and brine. The viscosity difference increases with increasing salinity. Under constant temperature and pressure conditions, the brine yield decreases with increasing salinity. Under the same pore volume CO_2 injection conditions, the residual saline in the maximum pore of the rock sample increases with increasing salinity. The probability of evaporation increases due to the increased probability of the brine coming into contact with the CO_2 flow and evaporating. However, changes in salinity can affect the balance between liquid water and water vapor. According to Raoult's law, as the salinity of a brine increases, the equilibrium vapor pressure (i.e., the

pressure exerted by the steam escaping from the liquid or solid) decreases, resulting in less evaporation. An experiment revealed that the amount of steam produced decreases with increasing salinity. The change in evaporation with increasing salinity exceeds the influence of the increase in the residual water saturation on the increase in evaporation (Fig. 9).

Furthermore, an increase in brine salinity increases the total dissolved solids. This directly increases the precipitation of salt. Thus, as the brine salinity increases, the interaction between reduced evaporation and increased total dissolved solids determines which interaction has the most significant effect on salt precipitation. Regarding the effect of brine salinity on the final permeability, an increase in brine salinity leads to a decrease in permeability and an increase in salt precipitation. The final gas phase measurement results show that the total dissolved solids content is the main factor controlling salting out due to changes in salinity.

It should be noted that the relative permeability curve for water is not sensitive to salinity (Javed et al., 2016). The main reason for this is that there is little difference in the brine yield under different salinity conditions (Javed et al., 2016). The low relative permeability of the nonwetting phase (CO_2) is due to pore throat obstruction caused by salt precipitation and the low CO_2/brine viscosity ratio. A lower injection rate and higher salinity will lead to more salt precipitation, reducing the difference in the relative permeability of CO_2.

In addition, the type of salt affects the trends of the changes in reservoir physical properties after CO_2 injection. The permeability decreases in cores saturated with NaCl and KCl brine. However, in $CaCl_2$ brine, redissolution is thought to be the main reason for increased permeability after $scCO_2$ injection (Mohammad et al., 2020).

Injection flow rate

The CO_2 injection flow rate plays a decisive role in the calculation of the injection capacity (Giorgis et al. 2007; He et al., 2024). The strength of the capillary force and convective force determines the influence of the injection flow rate (Dayo et al. 2021). A sensitivity analysis of the injection flow rate showed that the degree of salt precipitation is determined by the evaporation rate, and the evaporation rate is mainly controlled by the injection flow rate (Javad and Behzad 2016). The injection rate controls (1) the initial fluid ($scCO_2$ and brine) and final $scCO_2$ saturation, (2) the time from the start to the end of the precipitation, and (3) the amount of salt precipitated (Dayo et al. 2021).

Under strict advection conditions, a higher flow will enhance the viscous force, thus enhancing the immiscible

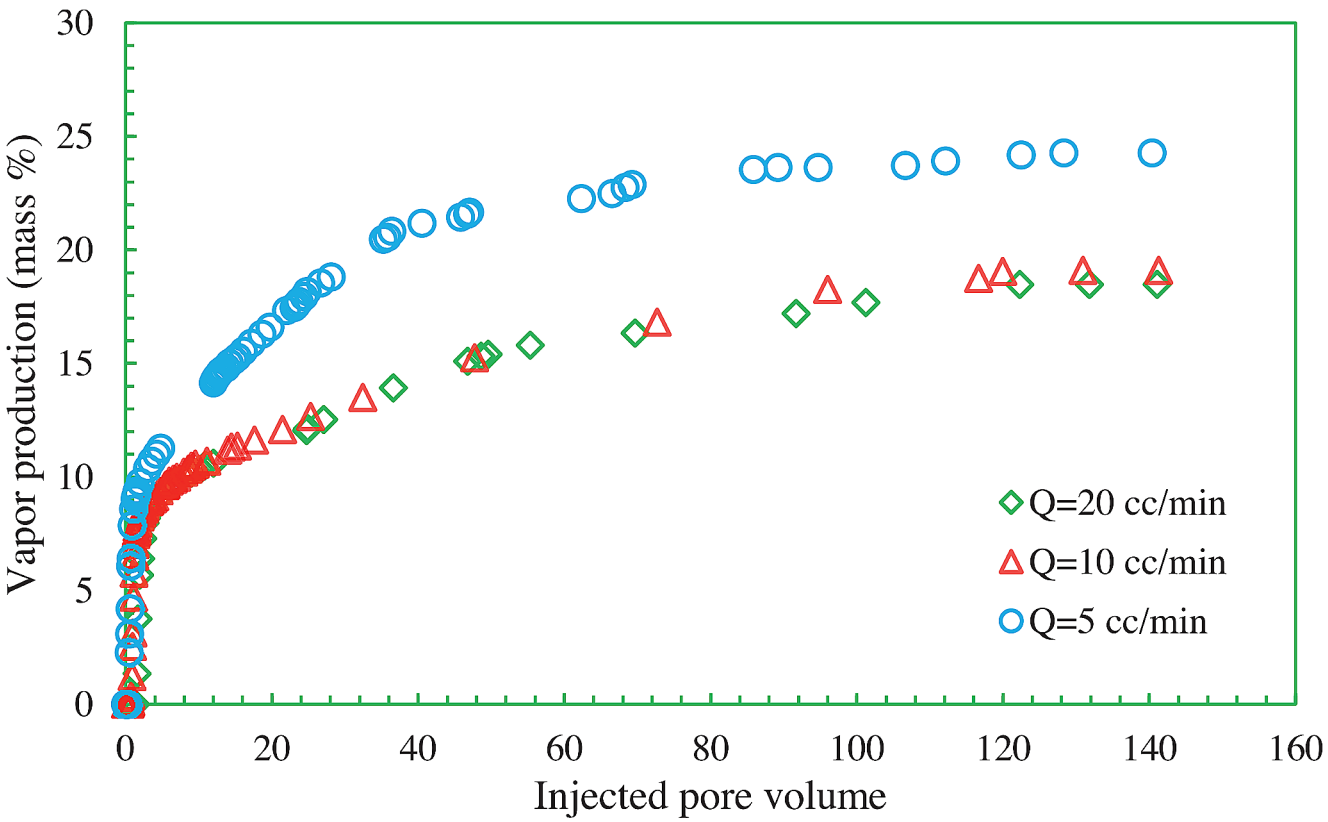

Fig. 9 Vapor production curves (Edited from Javed et al., 2016)

displacement of the $scCO_2$ at the pore scale. For $scCO_2$ injection and the same pore volume, the overall effect of a high injection flow rate is a decrease in the residual brine saturation (Dayo et al. 2021). Javed et al. (2016) concluded that as the injection flow rate increased, brine production increased, and the residual water saturation in the rock samples decreased with increasing injection flow rate (Fig. 10). Because the injection flow rate improves advection, the capillary forces in the medium can be more easily overcome. A decrease in the residual saturation will greatly reduce the amount of water molecules in the pore throats of the rock sample exposed to the CO_2 stream, and the probability of evaporation into water vapor will decrease.

When the injection flow rate increases, the evaporation rate increases (Javed and Behzad, 2016; Dayo et al. 2021). The evaporation front advances at a faster rate, leaving a uniform salt deposit in the dry zone. However, a lower injection flow rate results in a higher capillary backflow to the evaporation surface, which suppresses the effect of the pressure gradient. The enhanced capillary flow in turn increases the likelihood of dense salt accumulation near the inlet (Parvin et al. 2020). The combination of a higher $scCO_2$ injection flow rate (i.e., a higher evaporation rate) and a lower brine saturation, which can be obtained after critical $scCO_2$ saturation is reached, results in a shorter salt precipitation stage.

In addition, when the injection flow rate is faster, the CO_2 and brine are in a nonequilibrium state, resulting in much less water evaporation. Thus, the steam production resulting from salting-out decreases with increasing injection flow rate. Therefore, an increase in the injection flow rate can lead to permeability damage and a decrease in salt precipitation. Celia et al. (2016) reported that high evaporation rates limit the transport of solids to the outer surface, resulting in a more uniform distribution of precipitation. A low drying rate leads to strong solid accumulation on the outer surface of the porous medium. However, the small throat reduces solute transport and limits the accumulation of solids on the surface. Dayo et al. (2021) concluded that a higher injection flow rate increased the rate of salt precipitation but reduced the amount of salt precipitation. For the same injection flow rate, more salting-out occurs in reservoirs with greater reservoir heterogeneity. According to Norouzi et al. (2021), with increasing injection rate, the amount of precipitated salt and the damage to the permeability decrease significantly. He et al. (2023) reported that in upper and lower heterogeneous structures, salt precipitation had little effect on the injection capacity regardless of the CO_2 injection flow rate. When the CO_2 injection flow rate is low, the salt tends to settle in situ in the small pore structure and form a crystal structure. When the CO_2 injection flow rate is high, salt tends to precipitate in large pores and form a clustered structure. However, the size of the precipitated salt clusters is independent of the injection rate, and approximately 85% of the salt clusters fall within the pore throat range of 5×10^{-6}–1×10^{-3} mm^3,

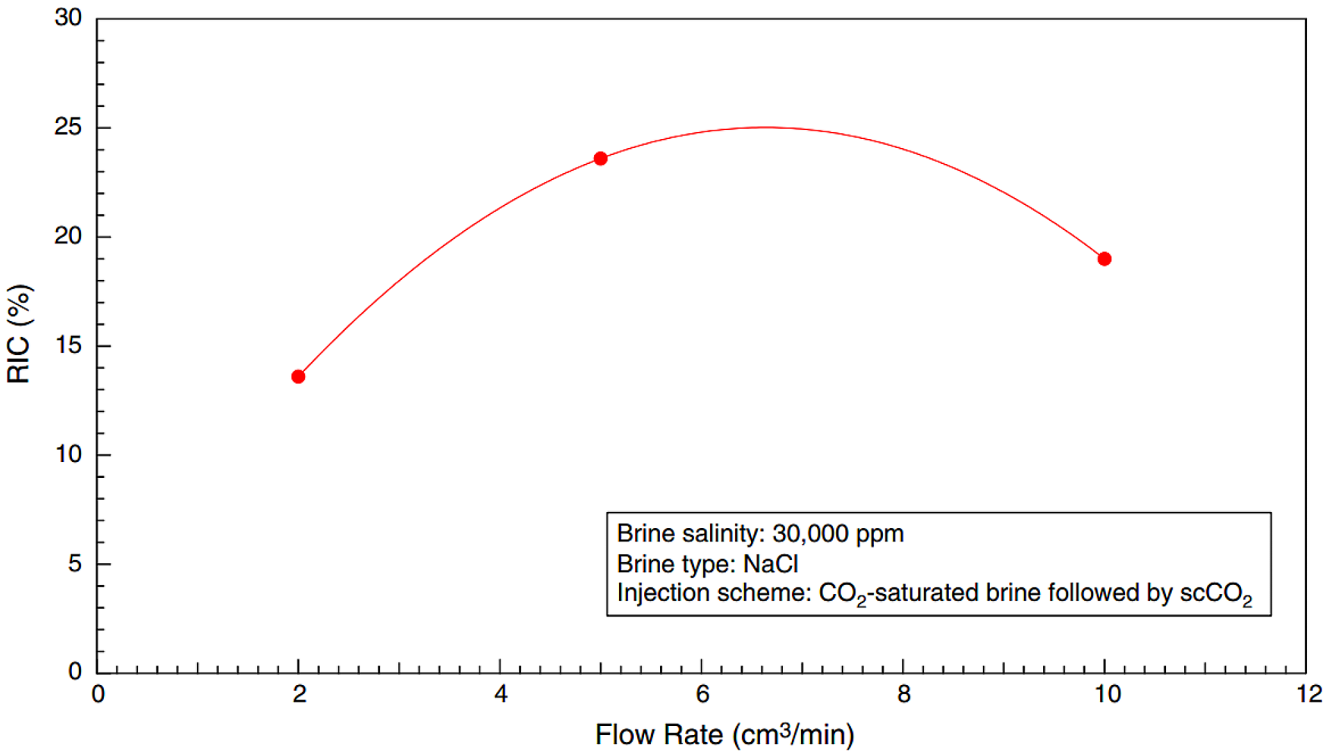

Fig. 10 Permeability changes measured on core samples before and after the coreflood experiment (Edited from Muhammad et al. 2020)

which means that they mostly form in connected medium pores (He et al. 2019).

The self-reinforcing mechanisms of salt growth and salt transport in water membranes must also be recognized (Miri et al. 2015). The aggregated salt crystals form microporous media (He et al. 2022), and each throat has highly capillary tubes that enhance solute transport by absorbing brine over long distances.

Temperature

In general, CO_2 is injected into the formation deeper than 850 m to ensure that the CO_2 is in a supercritical pressure and temperature state (Bachu 2008; Paluszny et al. 2020; Feng et al. 2023), which is likely to be lower than the original formation fluid temperature (Doughty and Freifeld 2013; Li and Zhang 2019). For instance, at the Cranfield pilot test site, the injected CO_2 temperature was 44 °C lower than the formation temperature (Kim and Hosseini 2014). The injection of CO_2 cools off the reservoir, especially in the near wellbore area, down to more than 30°C (Tang et al. 2018). The maximum solubility of salt in a brine solution and the phase behavior of a CO_2–brine system are mainly affected by temperature. Higher temperatures significantly increase the solubility of water in the CO_2 phase, thus increasing the rate of evaporation. As a result, water quickly reaches its saturation limit, and salts precipitate (Miri and Hellevang, 2016). The advancement of the drying front also accelerates with increasing temperature (Parvin et al. 2020). Additionally, elevated CO_2 temperature decreases the CO_2 density, enhancing the gravity override, which simultaneously proceeds to localized salt precipitation at the dry-out front (Kim et al. 2012).

The amounts and the time of the salt precipitation vary due to changes in injection temperature (Han et al. 2012). Increasing temperature increases the solubility of water in CO_2, capillary reflux and vaporization, which results in a stronger backflow intensity and a decrease in the time span of capillary-driven backflow (Norouzi et al. 2021). It could be observed that a rise in the injection temperature will cause an increase in the amount of precipitation and a reduction in porosity.

However, there exist different conclusions regarding the impact of the initial reservoir temperature on salting-out. Miri and Hellavang (2016) studied the effects of salinity, temperature, and initial reservoir permeability on salting-out through parameter analysis and demonstrated that the higher the salinity and temperature are, the lower the initial permeability of the reservoir, and the greater the likelihood of salt precipitation. Tang et al. (2018) performed the parametric analyses to explore the impacts of the initial reservoir temperature on salt precipitation. The outcomes demonstrated that the higher the temperature, the more intense the evaporation effect of the formation water would be, and the more prone to salt precipitation it was likely to be. Norouzi et al. (2021) compared the amount of water backflow and salt precipitation at different initial reservoir temperatures (Norouzi et al. 2021). It was inferred that the quantity of salt out diminishes along with the increase of the initial temperature. Concurrently, the initial temperature of the reservoir exerted a more significant effect compared to the CO_2 injection temperature. It was observed that with the rise of the initial reservoir temperature, the maximum value of backflow augmented and the time span decreased. Additionally, the lower the reservoir temperature was, the higher the salt precipitation rate would be and the greater the reduction in porosity tended to be.

In general, the influences of the aquifer temperature on the changes in the porosity and permeability caused by salt precipitation are not significant. The influences of a temperature change of 15 °C on the permeability and porosity are only 0.09% and 0.03%, respectively (Milad et al. 2017). The temperature largely changes the distribution of salt, but the degree of salt precipitation remains the same (Parvin et al. 2020). Nevertheless, it is likely that the influence of temperature on salt precipitation is significantly smaller than that of parameters like the injection rate and capillary pressure.

Furthermore, the relative permeability curve does not alter significantly within a small temperature range. This can account for the flow geometry limitations of one phase in relation to another in the majority of cases (Li and Liu, 2006). Experimental investigations have revealed that there is scarcely any change in the relative permeability curve within the temperature range of 90 to 120 °C (Peysson et al. 2014).

Wettability

The times of the beginning and end of salt precipitation during CO_2 injection are a function of the wettability and heterogeneity. The combination of greater water wetness and weaker reservoir heterogeneity will shorten the start-to-end period. In addition, the presence of stronger hydrophilic minerals can lead to more salt precipitation in near-well systems. This is because the proportion of hydrophilic pores is greater in a hydrophilic system than in a hydrophobic medium, and the brine connectivity is greater. He et al. (2019) observed that the distribution of salt in pores ranges from uniform clusters in hydrophilic systems to isolated large crystals in completely hydrophobic media. The latter is due to the poor hydraulic connectivity of the brine caused by the hydrophobicity of the pores, which limits the return of the solute to the evaporation site (He et al. 2019).

In practical engineering applications, wettability has been found to have an important effect on salt extraction behavior in reservoirs. Because of the low porosity and low permeability of highly heterogeneous sandstone reservoirs, fracturing and fracture-forming operations are often needed before CO_2 injection. Under hydrophilic conditions, salt easily precipitates in fractures, which seriously affects the injection capacity. Under hydrophobic conditions, salt hardly settles in fractures, which is very favorable for continuous CO_2 injection (He et al. 2022). Using a brine saturation micromodel characterized by matrix connection to a single fracture, Rufai and Crawshaw (2018) observed that salt precipitation and permeability reduction in both the matrix and fracture are controlled by wettability. The matrix permeability and fracture permeability decrease with the formation of salt precipitates in both water-wet micromodels and mixed wet micromodels. However, in the homogeneous hydrophobic micromodel, the lack of hydraulic connectivity of the brine phase limits the supply of solute to the fracture, and the fracture permeability decreases the least (Rufai and Crawshaw 2018). Iglauer (2017) stated that the injection of CO_2 into hydrophilic reservoir rocks is more advantageous because it improves the capture of residual CO_2, thereby improving the CO_2 storage capacity and the safety of long-term CO_2 storage. An ideal CO_2-sealed storage layer is one in which the reservoir rock near the injection well is hydrophobic, which improves the injection capacity, and the remote reservoir rocks are hydrophilic, which improves the reservoir capacity. Manual methods can be used to modify the wettability of fractures near injection wells. For example, the fracture surface can be made hydrophobic by injecting a surface-modifying solvent.

Implications and problems of research on CO_2 storage salt precipitation in saline sandstone

The influence of chemical reactions

As shown in Table 3, the following chemical reactions occur in sandstone aquifers (Milad et al. 2017; Zhang et al., 2024). Various types of minerals, such as carbonate, feldspar, and clay, will experience chemical reactions to varying degrees after contact with weakly acidic fluids formed by CO_2 and formation water (Edgar et al. 2023). These chemical reactions alter the porosity and permeability of the rock (Cui et al. 2018b). Nevertheless, the conclusions regarding the variation characteristics and magnitude of porosity and permeability are not uniform.

By summarizing the previous research results, the reasons for the significant differences in porosity and permeability are as follows. (1) The core samples utilized in the experiments had diverse mineral compositions. (2) The temperature and pressure setting of each experiment were different. (3) The durations of time were dissimilar in the majority of experiments, and most experiments were restricted to short-term effects, not revealing anything about the long-term effects of CO_2 reaction (Rathnaweera et al. 2017). It should be noted that the reaction rate of different minerals vary by several orders of magnitude (Balashov et al. 2013; Zhang et al., 2017). Concurrently, mineral dissolution may be accompanied by the generation of secondary minerals, which may migrate and block the pores, thereby resulting in the reduction of porosity and permeability. More studies have discovered that in the early stage of CO_2 injection, minerals such as carbonate and feldspar dissolve with the decrease of formation water PH value (Feng et al. 2023). The dissolution increases the concentration of Ca^{2+} and Mg^{2+} ions. They react with the available carbonate ions in

Table 3 Chemical reaction between CO_2 water solution and certain minerals (edited from Milad et al. 2017; Zhang et al., 2024)

Mineral type	Mineral names	Chemical formula	The chemical reactions with CO_2 water solution
Carbonate	Calcite	$CaCO_3$	$CaCO_3+CO_2+H_2O\rightarrow Ca(HCO_3)_2$
	Dolomite	$CaR(CO_3)_2$	$CaR(CO_3)_2+2CO_2+2H_2O\rightarrow Ca(HCO_3)_2+R(HCO_3)_2$
	Magnesite, Siderite, Rhodochrosite	$R(CO_3)_2$	$R(CO_3)_2+CO_2+H_2O\rightarrow R(HCO_3)_2$
Feldspar	Sodium Feldspar	$NaAlSi_3O_8$	$2NaAlSi_3O_8+2CO_2+3H_2O\rightarrow Al_2Si_2O_5(OH)_4+2Na^++4SiO_4+2HCO_3^-$, $NaAlSi_3O_8+CO_2+H_2O\rightarrow NaAlCO_3(OH)_2+3SiO_4$
	Calcium Feldspar	$CaAl_2Si_2O_8$	$CaAl_2Si_2O_8+2CO_2+3H_2O\rightarrow Al_2Si_2O_5(OH)_4+CaCO_3$
	Potassium Feldspar	$KAlSi_3O_8$	$2KAlSi_3O_8+2CO_2+3H_2O\rightarrow Al_2Si_2O_5(OH)_4+2\ K^++4SiO_4+2HCO_3^-$
Clay	Illite	$K_{0.6}Mg_{0.25}Al_{2.3}Si_{3.5}O_{10}(OH)_2$	$K_{0.6}Mg_{0.25}Al_{2.3}Si_{3.5}O_{10}(OH)_2+8\ H^+\rightarrow 5H_2O+0.6\ K^++0.25Mg^{2+}+2.3\ Al^{3+}+3.5SiO_2$
	Chlorite	$A_5Al_2Si_3O_{10}(OH)_8$	$A_5Al_2Si_3O_{10}(OH)_8+5CaCO_3+5CO_2\rightarrow 5CaA(CO_3)_2+Al_2Si_2O_5(OH)_4+SiO_2+2H_2O$
	Kaolinite	$Al_4Si_4O_{10}(OH)_8$	$3Al_4Si_4O_{10}(OH)_8+4K^++4HCO_3^-\rightarrow 4KAl_3Si_3O_{10}(OH)_2+4CO_2+10H_2O$

Note R represents Mg/Fe/Mn, and A represents Mg/Fe

the formation to form calcium carbonate or calcite deposits (Zhang et al. 2019a).

More importantly, it is essential to identify the distinctions among various chemical reactions and salting-out effects in the course of discussing the alterations in porosity, permeability and injectivity of the saline sandstone.

The relationship between salt precipitation and reservoir porosity/permeability changes

A variety of studies, relying on both simulation and field data, observed salt precipitation and its detrimental impacts on the reservoir. Salt could deposited in both macro-pores and micro-pores (Akindipe et al., 2021). The accumulation of salt deposits within the pore space of reservoir rocks leads to a decrease in porosity, which is directly associated with the decline in permeability as theorized by the permeability-porosity relationships in the relevant literature (Verma and Pruess, 1988; Pruess 2009).

However, in diverse experiments and field data, the quantitative relationship between salt precipitation and the alterations in reservoir porosity and permeability is not consistent. Baumann et al. (2014) reported a salt saturation of approximately 1.4% within the dry-out region, with the maximal saturation reaching up to 14.1%. Muller et al. (2009) observed a solid salt precipitation of around 16% and a consequent permeability reduction of approximately 40%. Bacci et al. (2011) detected a reduction in porosity ranging from 3 to 5% and a permeability reduction ranging from 13 to 75%. Tang et al. (2014) reported a reduction of 14.6% and 83.3% in porosity and permeability respectively in their model. Grimm et al. (2020) reported a 21.98% permeability reduction in their studies. Ott et al. (2021) probed into the potential influence of salt precipitation on reservoir permeability, and the results indicated that the reservoir permeability decreased by up to three orders of magnitude due to salt precipitation. Zhang et al. (2019a) carried out the core evaporation test to explore the change in permeability caused by salt precipitation, and the results showed that the core permeability decreased by up to 90% because of the continuous salt precipitation.

Consequently, the establishment of a more precise mathematical model for the alterations of porosity, permeability, and injectivity brought about by salting out is a vital task for the storage of CO_2 in saline sandstone reservoirs.

Reservoir heterogeneity has a profound effect on salt precipitation during CO_2 sequestration

Reservoir heterogeneity is a key factor affecting CO_2 transport, reservoir capacity, and storage efficiency. Several recent studies have discussed the effects of heterogeneity on CO_2 migration and storage through a combination of core displacement tests and numerical simulations (Norouzi et al. 2022). In contrast to marine carbonate strata, continental clastic strata exhibit greater reservoir heterogeneity. The poor spatial continuity of the sand bodies, the obvious low porosity and low permeability characteristics of the reservoirs, and the presence of mud interlayers further aggravate the risk of salt precipitation in the process of CO_2 storage and affect the CO_2 injection effect. In future research, more attention needs to be given to the influence of reservoir heterogeneity on CO_2 storage salt precipitation from the aspects of macro- and micro-reservoir heterogeneity.

Is there an optimal injection rate

The injection rate is one of the few parameters that can be controlled in the field. Is there an optimal injection rate? Ott et al. (2013) combined experiments and numerical simulations to determine that different CO_2 injection rates produce precipitates with different forms. There is a critical flow rate q_{cr} during CO_2 injection. When the CO_2 flow rate is below q_{cr}, a negative water saturation gradient may occur. More water dissolves/evaporates near the injection point. This results in a return flow of brine driven by capillary action toward the injection point, where a large amount of local precipitation occurs. As a result, the amount of locally precipitated salt may be greater than the amount of salt originally dissolved in the saline phase, which will most likely clog the pore space. When the injection rate reaches q_{cr}, the capillary reflux phenomenon stops, and the local precipitation phenomenon at the injection point disappears. The critical volume flow q_{cr} can be determined via mass balance. Peysson et al. (2014) believed that there was a critical flow rate beyond which the dry front would spread uniformly along the flow direction and the salt would precipitate uniformly. At high injection rates, the viscous force increases, and the capillary force weakens. At a flow rate of 4.4 ml/min, the uniform salt saturation of the entire core after drying was 0.04. However, such experimental data are scarce, and heterogeneous salt precipitation has been observed in most experiments (Peysson et al. 2014; André et al. 2014; Ott et al. 2015).

Therefore, if an optimal injection rate can be determined or a method can be found to quickly estimate the optimal injection rate according to the on-site geological conditions, it is highly important to reduce the injectable damage caused by salt precipitation and to improve the effect of CO_2 injection.

NaCl does not represent all of the actual salt precipitation in the subsurface

In addition to Na^+ and Cl^-, saline sandstone also contains other inorganic ions, such as K^+, Ca^{2+}, Mg^{2+}, SO_4^{2-}, and HCO_3^-. These inorganic ions also precipitate under the action of water evaporation (He et al. 2024b). Moreover, these inorganic ions can react with dissolved CO_2, resulting in mineral precipitation or mineral dissolution. Ueda et al. (2005), Cui et al. (2017), and Xu et al. (2014) analyzed the water–rock geochemical reactions of CO_2 generation through geochemical experiments and numerical simulations and found that the mineral dissolution caused by CO_2 geochemical reactions was negligible during CO_2 injection. However, under the action of water evaporation, mineral precipitation intensifies. At present, most experiments and numerical simulations conducted to simulate the salt precipitation process have utilized NaCl, and the setting of the brine properties is too simple. In fact, the mineral composition of CO_2-sequestration formation water is complex, and the impact of this difference in the composition of the brine needs to be considered.

In addition, the reasons for the formation of different forms of NaCl crystals are still unclear, and the main factors controlling salt crystallization are still unclear. Since the quantitative relationship between the $scCO_2$ flow and NaCl precipitation in different pore structures has not been established, it is difficult to predict the actual amount and location of NaCl precipitation in the pores. Therefore, it is still necessary to analyze the salt crystallization kinetics of $scCO_2$ injected into saline aquifers.

5.6 How can the results of core experiments and numerical simulations be better applied to field CO_2 injection applications.

It has always been the goal of researchers to reconstruct underground geology as accurately as possible to improve the applicability of the results of core experiments and numerical simulations. Some studies have used seismic data and multiwell drilling information to create reservoir heterogeneity models (Qing et al., 2021; Deng et al. 2012). However, there are still some challenges, including how to leverage the parameters obtained from core studies to the reservoir/saline aquifer scale under formation conditions and how to conduct simulation studies using field data. Due to the lack of in situ data, most laboratory experiments have failed to fully restore the actual heterogeneity of underground strata. The next step in such research will be to conduct further specific studies using a combination of core sample analysis, numerical simulations, and field investigations (Xiao et al. 2019).

Summary and conclusions

A great number of numerical simulations, core tests, and analytical models have been carried out to investigate the salting-out effect in saline aquifers, and the main understandings obtained are as follows. (1) After the injection of $scCO_2$ into a saline aquifer, the synergistic coupling of viscous displacement and drying results in three physical processes: immiscible two-phase displacement, the evaporation of brine into a dry CO_2 flow, and capillary-driven water phase backflow. (2) Laboratory experiments, numerical simulations and analytical models are capable of offering visual and swift analyses of the characteristics and causes of salt precipitation.

However, the current research regarding salt precipitation is far from enough, and the following aspects remain ambiguous. (1) The current core experiments, numerical simulations, and analytical models do not comprehensively encompass the pressure, temperature, and salinity conditions related to long-term CO_2 injection. (2) The location, distribution, and dynamic mechanism of salting-out in saline aquifers are still not well-defined. (3) The quantitative relationship among various factors with respect to the salting-out effect is not clear.

Some key scientific issues need to be addressed to accurately predict salt precipitation in saline sandstone. (1) Once CO_2 and formation water establish weakly acidic fluid contact, varying degrees of chemical reactions will take place. These chemical reactions alter the porosity and permeability of the rock. It is necessary to distinguish between these chemical reactions and the changes in injectivity brought about by salting-out. (2) In comparison with carbonate rocks, continental clastic rocks are more heterogeneous, and this disparity will have a more significant impact on salting-out. (3) The prevailing academic view is that there exists an optimal injection rate. This optimal injection rate requires confirmation through more core experiments, analytical models, numerical simulation results, and field practices. (4) The setting of brine in the present study is overly simplistic, being restricted to NaCl, and more complex brine mineral composition as well as salt crystallization kinetics need to be taken into consideration. (5) There are certain differences between the results of core experiments, numerical simulations, and the actual underground geological conditions, which may result in incorrect estimations of the injectivity loss caused by salting-out.

Acknowledgements This study was financially supported by the Open Fund of the State Key Laboratory of Shale Oil and Gas Enrichment Mechanisms and Effective Development (G5800-20-ZSK-FGY009), the National Natural Science Foundation of China (Grant No. 42102184), and the National Science and Technology Innovation Training Program for College Students (202311551019).

Author contributions Luo Chao and Lisongze wrote the main manuscript text and Yuan Jialin prepared Figs. 1, 2, 3, 4, 5, 6, 7, 8 and 9. All authors reviewed the manuscript.

Data availability No datasets were generated or analysed during the current study.

Declarations

Competing interests The authors declare no competing interests.

References

André L, Peysson Y, Azaroual M (2014) Well injectivity during CO_2 storage operations in deep saline aquifers—part 2: numerical simulations of drying, salt deposit mechanisms and role of capillary forces. Int J Greenh Gas Con 22:301–312

Babak S, Javier V (2018) A fast and robust TOUGH2 module to simulate geological CO_2 storage in saline aquifers. Comput Geosci 111:58–66

Bacci G, Korre A, Durucan S (2011a) An experimental and numerical investigation into the impact of dissolution/precipitation mechanisms on CO_2 injectivity in the wellbore and far field regions. Int J Greenh Gas Con 5(3):579–588

Bacci G, Korre A, Durucan S (2011b) Experimental investigation into salt precipitation during CO_2 injection in saline aquifers. Energy Procedia 4:4450–4456

Bachu S (2008) CO_2 storage in geological media: role, means, status and barriers to deployment. Prog Energ Combust 34:254–273

Balashov VN, Guthrie GD, Hakala JA et al (2013) Predictive modeling of CO_2 sequestration in deep saline sandstone reservoirs: impacts of geochemical kinetics. Appl Geochem 30:41–56

Baumann G, Henninges J, Lucia MD (2014) Monitoring of saturation changes and salt precipitation during CO_2 injection using pulsed neutron-gamma logging at the Ketzin pilot site. Int J Greenh Gas Con 28:134–146

Celia MA, Nordbotten JM, Court B et al (2011) Field-scale application of a semianalytical model for estimation of CO_2 and brine leakage along old wells. Int J Greenh Gas Con 5(2):257–269

Chen XS, Hu R, Zhou CX et al (2024) Capillary-driven backflow during salt precipitation in a rough fracture. Water Resour Res 60(3): e2023WR035451

Cui GD, Zhang L, Ren B et al (2016a) Geothermal exploitation from depleted high temperature gas reservoirs by recycling supercritical CO_2: heat mining rate and salt precipitation effects. Appl Energ 183:837–852

Cui GD, Ren S, Zhang L et al (2016b) Formation water evaporation induced salt precipitation and its effect on gas production in high temperature natural gas reservoirs. Petrol Explor Dev 43(5):749–758

Cui GD, Zhang L, Tan C (2017) Injection of supercritical CO_2 for geothermal exploitation from sandstone and carbonate reservoirs: CO_2–water–rock interactions and their effects. J CO_2 Util 20:113–128

Cui GD, Ren S, Rui Z (2018a) The influence of complicated fluid-rock interactions on the geothermal exploitation in the CO_2 plume geothermal system. Appl Energ 227:49–63

Cui GD, Wang Y, Rui Z et al (2018b) Assessing the combined influence of fluid-rock interactions on reservoir properties and injectivity during CO_2 storage in saline aquifers. Energy 155:281–296

Cui GD, Hu Z, Ning FL et al (2023) A review of salt precipitation during CO_2 injection into saline aquifers and its potential impact on carbon sequestration projects in China. Fuel 334:126615

Dayo A, Soheil S, Mohammad P (2021) Salt precipitation during geological sequestration of supercritical CO_2 in saline aquifers: a pore-scale experimental investigation. Adv Water Resour 155:104011

Dayo A, Soheil S, Mohammad P (2022) Salt precipitation in carbonates during supercritical CO_2 injection: a pore-scale experimental investigation of the effects of wettability and heterogeneity. Int J Greenh Gas Con 121:103790

Deng HL, Stauffer PH, Dai ZX et al (2012) Simulation of industrial-scale CO_2 storage: multiscale heterogeneity and its impacts on storage capacity, injectivity and leakage. Int J Greenh Gas Con 10:397–418

Doughty C, Freifeld BM (2013) Modeling CO_2 injection at Cranfield, Mississippi: investigation of methane and temperature effects. Greenh Gases 3:475–490

Edem D, Abba M, Nourian A et al (2020) Experimental Investigation of the Extent of the Impact of Halite Precipitation on CO_2 Injection in Deep Saline Aquifers. SPE Europec featured at 82nd EAGE Conference and Exhibition

Edgar B, Timea K, Gricelda HF et al (2023) Laboratory studies on CO_2-brine-rock interaction: an analysis of research trends and current knowledge. Int J Greenh Gas Con 123:103842

Emad AA, Stephanie V, Ahmed B et al (2017) Effect of brine salinity on CO_2 plume migration and trapping capacity in deep saline aquifers. APPEA J 57:100–109

Feng Y, Zhang S, Ma C et al (2023) The role of Geomechanics for Geological Carbon Storage. Gondwana Res 124:100–123

Flemisch B, Darcis M, Erbertseder K et al (2011) DuMux: DUNE for multi{phase, component, scale, physics,… flow and transport in porous media. Adv Water Resour 34:1102–1112

Fujimaki H, Shimano T, Inoue M et al (2006) Effect of a salt crust on evaporation from a bare saline soil. Vadose Zone J 5:1246–1256

Giacomo B, Anna K, Sevket D (2011) Experimental investigation into salt precipitation during CO_2 injection in saline aquifers. Energy Procedia 4:4450–4456

Giorgis T, Carpita M, Battistelli A (2007) 2D modeling of salt precipitation during the injection of dry CO_2 in a depleted gas reservoir. Energ Convers Manage 48(6):1816–1826

Golghanddashti H, Saadat M, Abbasi S et al (2013) Experimental investigation of water vaporization and its induced formation damage associated with underground gas storage. J Porous Media 16(2):89–96

Grimm LM, Schädle P, Green CP et al (2020) Permeability impairment and salt precipitation patterns during CO_2 injection into single natural brine-filled fractures. Water Resour Res 56(8): e2020WR027213

Grude S, Landrø M, Dvorkin J (2014) Pressure effects caused by CO_2 injection in the Tubåen Fm, the Snøhvit field. Int J Greenh Gas Con 27:178–187

Han WS, Kim KY, Park E et al (2012) Modeling of spatiotemporal thermal response to CO_2 injection in saline formations: interpretation for monitoring. Transp Porous Med 93:381–399

Hassan D, Nima S, Muhammad S (2018) Pore-network model of evaporation-induced salt precipitation in porous media: the effect of correlations and heterogeneity. Adv Water Resour 112:59–71

He D, Jiang PX, Xu RN (2019) Pore-scale experimental investigation of the effect of supercritical CO_2 injection rate and surface wettability on salt precipitation. Environ Sci Technol 53(24):14744–14751

He D, Xu RN, Ji TC, Jiang PX (2022) Experimental investigation of the mechanism of salt precipitation in the fracture during CO_2 geological sequestration. Int J Greenh Gas Con 118:103693

He D, Jiang PX, Xu RN (2023) The influence of heterogeneous structure on salt precipitation during CO_2 geological storage. Adv Geo-Energy Res 7(3):189–198

He D, Wang Z, Yuan H et al (2024a) Experimental investigation of salt precipitation behavior and its impact on injectivity under variable injection operating conditions. Gas Sci Eng 121:205198

He YW, Wang N, Tang Y et al (2024b) Formation-water evaporation and salt precipitation mechanism in porous media under movable water conditions in underground gas storage. Energy 286:129532

Huinink HP, Pel L, Michels M (2002) How ions distribute in a drying porous medium: a simple model. Phys Fluids 14(4):1389–1395

Iglauer S (2017) CO_2-water–rock wettability: variability, influencing factors, and implications for CO_2 geostorage. Acc Chem Res 50(5):1134–1142

Izgec O, Demiral B, Bertin H et al (2008) CO_2 injection into saline carbonate aquifer formations I: laboratory investigation. Transp Porous Media 72(1):1–24

Javad J, Behzad R (2016) Experimental investigation of injectivity alteration due to salt precipitation during CO_2 sequestration in saline aquifers. Adv Water Resour 96:23–33

Jiang S, Zhang K, Du FS et al (2023) Progress and prospects of CO_2 storage and enhanced oil, gas and geothermal recovery. Earth Sci : 1–22

Kelly HL, Mathias SA (2018) Capillary processes increase salt precipitation during CO_2 injection in saline formations. J Fluid Mech 852:398–421

Kim S, Hosseini SA (2014) Above-zone pressure monitoring and geomechanical analyses for a field-scale CO_2 injection project in Cranfield, MS. Greenh Gases 4:81–98

Kim KY, Han WS, Oh J (2012) Characteristics of salt-precipitation and the associated pressure build-up during CO_2 storage in saline aquifers. Transp Porous Media 92(2):397–418

Kim M, Sell A, Sinton D (2013) Aquifer-on-a-chip: understanding pore-scale salt precipitation dynamics during CO_2 sequestration. Lab Chip 13(13):2508–2518

Kleinitz W, Koehler M, Dietzsch G (2001) The precipitation of salt in gas producing wells. SPE 68953:21–22

Lehmann P, Or D (2009) Evaporation and capillary coupling across vertical textural contrasts in porous media. Phys Rev E 80:046318

Lehmann P, Assouline S, Or D (2008) Characteristic lengths affecting evaporative drying of porous media. Phys Rev E 77:056309

Li S, Zhang D (2019) How effective is carbon dioxide as an alternative fracturing fluid? SPE J 24:857–876

Li X, Liu Y, Bai B (2006) Ranking and screening of CO_2 saline aquifer storage zones in China. Chin J Rock Mech Eng 25(5):963–968

Liu HH, Zhang G, Yi Z (2013) A permeability-change relationship in the dryout zone for CO_2 injection into saline aquifers. Int J Greenh Gas Con 15:42–47

Liu DQ, Li YL, Song SY (2016) Simulation and analysis of lithology heterogeneity on CO_2 geological sequestration in deep saline aquifer: a case study of the Ordos Basin. Environ Earth Sci 75:962–975

Mathias SA, Gluyas JG, González M et al (2011) Role of partial miscibility on pressure buildup due to constant rate injection of CO_2 into closed and open brine aquifers. Water Resour Res 47(12):W12525

Mehdi Z, Mehran PD, David K (2009) Analytical solution to evaluate salt precipitation during CO_2 injection in saline aquifers. Int J Greenh Gas Con 3:600–611

Meng QL, Jiang X, Li DD et al (2015) Numerical simulations of pressure buildup and salt precipitation during carbon dioxide storage in saline aquifers. Comput Fluids 08:012

Milad G, Seyyed AT, Elnaz K (2017) Modeling rock–fluid interactions due to CO_2 injection into sandstone and carbonate aquifer considering salt precipitation and chemical reactions. J Nat Gas Sci Eng 37:523–538

Miri R, Hellavang H (2016) Salt precipitation during CO_2 storage: a review. Int J Greenh Gas Con 51:136–147

Miri R, Noort VR, Aagaard P et al (2015) New insights on the physics of salt precipitation during injection of CO_2 into saline aquifers. Int J Greenh Gas Con 43:10–21

Muhammad AMY, Mohamad AI, Mazlin I (2020) Effects of CO2/Rock/Formation brine parameters on CO_2 injectivity for sequestration. SPE J: 203843

Muller N, Qi R, Mackie E (2009) CO_2 injection impairment due to halite precipitation. Energy Procedia 1(1):3507–3514

Noh MH, Lake LW, Bryant SL et al (2007) Implications of coupling fractional flow and geochemistry for CO_2 injection in aquifers. SPE Reserv Eval Eng 10(04):406–414

Nooraiepour M, Fazeli H, Miri R (2018) Effect of CO_2 phase states and flow rate on salt precipitation in shale caprocks—a microfluidic study. Environ Sci Technol 52(10):6050–6060

Nordbotten JM, Celia MA (2006) Similarity solutions for fluid injection into confined aquifers. J Fluid Mech 561:307–327

Norouzi AM, Babaeia M, Han W (2021) CO_2-plume geothermal processes: a parametric study of salt precipitation influenced by capillary-driven backflow. Chem Eng J 425:130031

Norouzi AM, Niasar V, Gluyas JG et al (2022) Analytical solution for predicting salt precipitation during CO_2 injection into saline aquifers in presence of capillary pressure. Water Resour Res 10:1029

Oh J, Kim KY, Han WS (2013) Experimental and numerical study on supercritical CO_2/brine transport in a fractured rock: implications of mass transfer, capillary pressure and storage capacity. Adv Water Res 62:442–453

Ott H, Kloe DK, Marcelis F et al (2011) Injection of supercritical CO_2 in brine saturated sandstone: pattern formation during salt precipitation. Energy Procedia 4:4425–4432

Ott H, Snippe J, Kloe DK et al (2013) Salt precipitation due to sc-gas injection: single versus multiporosity rocks. Energy Procedia 37:3319–3330

Ott H, Andrew M, Snippe J et al (2014) Microscale solute transport and precipitation in complex rock during drying. Geophys Res Lett 41:8369–8376

Ott H, Roels SM, Kloe DK (2015) Salt precipitation due to supercritical gas injection: I Capillary-driven flow in unimodal sandstone. Int J Greenh Gas Con 43:247–255

Ott H, Snippe J, Kloe DK (2021) Salt precipitation due to supercritical gas injection: II capillary transport in multi porosity rocks. Int J Greenh Gas Con 105:103233

Paluszny A, Graham CC, Daniels KA et al (2020) Caprock integrity and public perception studies of carbon storage in depleted hydrocarbon reservoirs. Int J Greenh Gas Con 98:103057

Parvin S, Masoudi M, Sundal A et al (2020) Continuum scale modeling of salt precipitation in the context of CO_2 storage in saline aquifers with MRST compositional. Int J Greenh Gas Con 99:103075

Peysson Y (2012) Permeability alteration induced by drying of brines in porous media. Eur Phys J Appl Phys 60:24206

Peysson Y, Bazin B, Magnier C et al (2011) Permeability alteration due to salt precipitation driven by drying in the context of CO_2 injection. Energy Procedia 4:4387–4394

Peysson Y, André L, Azaroual M (2014) Well injectivity during CO_2 storage operations in deep saline aquifers—part 1: experimental investigation of drying effects, salt precipitation and capillary forces. Int J Greenh Gas Con 22:291–300

Pruess K (1991) TOUGH2-A General-purpose Numerical Simulator. for Multiphase Fluid and Heat Flow

Pruess K (2005) ECO_2N: a TOUGH2 fluid property module for mixtures of water, NaCl, and CO_2. Lawrence Berkeley National Laboratory, Calif, Berkeley, CA

Pruess K (2009) Formation dry-out from CO_2 injection into saline aquifers: part 2, Analytical model for salt precipitation. Water Resour Res 45(3):W03403

Pruess K, Spycher N (2007) Eco_2n – a fluid property module for the tough2 code for studies of CO_2 storage in saline aquifers. Energ Convers Manage 48(6):1761–1767

Qanbari F, Pooladi DM, Tabatabaie SH et al (2012) CO_2 disposal as hydrate in ocean sediments. J Nat Gas Sci Eng 8:139–149

Qing XX, Fekri M (2021) Determination on pore size distribution by a probabilistic porous network subjected to salt precipitation and dissolution. Comp Mater Sci 195:110491

Qiu YN (1992) Developments in reservoir sedimentology of continental clastic rocks in China. Acta Sedimentol Sin 10(3):16–23

Rathnaweera TD, Ranjith PG, Perera MSA et al (2017) An experimental investigation of coupled chemico-mineralogical and mechanical changes in varyingly-cemented sandstones upon CO_2 injection in deep saline aquifer environments. Energy 133:404–414

Ren J, Wang Y, Feng D et al (2021) CO_2 migration and distribution in multiscale-heterogeneous deep saline aquifers. Adv Geo-Energy Res 5(3):333–346

Roels SM, Ott H, Zitha PL (2014) μ-CT analysis and numerical simulation of drying effects of CO_2 injection into brine-saturated porous media. Int J Greenh Gas Con 27:146–154

Rufai A, Crawshaw J (2018) Effect of wettability changes on evaporation rate and the permeability impairment due to salt deposition. ACS Earth Space Chem 2(4):320–329

Shokri N (2014) Pore-scale dynamics of salt transport and distribution in drying porous media. Phys Fluids 26:012106

Smith MM, Sholokhova Y, Hao Y et al (2013) CO_2-induced dissolution of low permeability carbonates part I: characterization and experiments. Adv Water Resour 62:370–387

Sokama N, Ursin JR (2018) The coupled effect of salt precipitation and fines mobilization on CO_2 injectivity in sandstone. Greenh Gases Sci Technol 8(6):1066–1078

Spycher N, Pruess K, Ennis KJ (2003) CO_2-H_2O mixtures in the geological sequestration of CO_2 I Assessment and calculation of mutual solubilities from 12 to 100 C and up to 600 bar. Geochim Cosmochim Acta 67(16):3015–3031

Tambach T, Loeve D, Hofstee C et al (2015) Effect of CO_2 injection on brine flow and salt precipitation after gas field production. Transp Porous Media 108(1):171–183

Tang Y, Yang R, Du Z et al (2015) Experimental study of formation damage caused by complete water vaporization and salt precipitation in sandstone reservoirs. Transp Porous Media 107(1):205–218

Tang Y, Yang R, Kang X (2018) Modeling the effect of water vaporization and salt precipitation on reservoir properties due to carbon dioxide sequestration in a depleted gas reservoir. Petrol 4:385–397

Ueda A, Kato K, Ohsumi T (2005) Experimental studies of CO_2-rock interaction at elevated temperatures under hydrothermal conditions. Geochem J 39(5):417–425

Wang Y, Liu Y (2014) Dry-out effect and site selection for CO_2 storage in deep saline aquifers. Rock Soil Mech 35(6):1711–1718

Wang Y, Mackie E, Rohan J et al (2009) Experimental study on halite precipitation during CO_2 sequestration. International Symposium of the Society of Core Analysts, Noordwijk. Netherlands: 27–30

Wang Z, Chen S, Yuan H et al (2023) Experimental investigation on salt precipitation behavior during Carbon Geological Sequestration: considering the influence of formation boundary solutions. Energ Fuel 38(1):514–525

Xiao T, McPherson B, Esser R et al (2019) Forecasting commercial-scale CO_2 storage capacity in deep saline reservoirs: Case study of Buzzard's bench, Central Utah. Comput Geosci 126:41–51

Xu T, Feng G, Shi Y (2014) On fluid–rock chemical interaction in CO_2-based geothermal systems. J Geochem Explor 144:179–1119

Xu R, Ji TC, Lu TJ et al (2022) Research progress on heat and mass transfer in carbon geological storage and enhanced oil/gas/geothermal recovery technology. J Tsingh Univ 62(4):634–654

Zeidouni M, Pooladi DM, Keith D (2009) Analytical solution to evaluate salt precipitation during CO_2 injection in saline aquifers. Int J Greenh Gas Con 3(5):600–611

Zhang S, Depaolo DJ (2017) Rates of CO_2 mineralization in geological carbon storage. Acc Chem Res 50(9):2075–2084

Zhang S, Liu HH (2016) Porosity–permeability relationships in modeling salt precipitation during CO_2 sequestration: review of conceptual models and implementation in numerical simulations. Int J Greenh Gas Con 52:24–31

Zhang L, Wang Y, Miao X et al (2019a) Geochemistry in geologic CO_2 utilization and storage: a brief review. Adv Geo-Energy Res 3:304–313

Zhang YZ, Zhang ML, Mei HY (2019b) Study on salt precipitation induced by formation brine flow and its effect on a high-salinity tight gas reservoir. J Petrol Sci Eng 183:106384

Zhang H, Sun Z, Zhang N et al (2024a) Brine drying and salt precipitation in porous media: a Microfluidics Study. Water Resour Res 60(1): e2023WR035670

Zhang LH, Zhang T, Zhao YL et al (2024b) A review of interaction mechanisms and microscopic simulation methods for CO_2-water-rock system. Petrol Explor Dev 51(1):223–238

Zhou QL, Birkholzer JT, Tsang CF (2008) A method for quick assessment of CO_2 storage capacity in closed and semiclosed saline formations. Int J Greenh Gas Con 2:626–639

Zuluaga E, Lake LW (2008) Modeling of experiments on water vaporization for gas injection using traveling waves. SPE J 13(02):248–256

Zuluaga E, Monsalve JC (2003) Water vaporization in gas reservoirs In: Paper SPE 84829-MS presented at the SPE Eastern Regional Mtng, 6–10 September, Pittsburgh, Pennsylvania 102118/84829-MS